THE ROLE OF THE CYTOCHROME *B* AND CYTOCHROME *C* OXIDASE III GENES IN THE IMMUNE RESPONSE OF THE SOUTH AFRICAN ABALONE, *HALIOTIS MIDAE*

BY

Marike Janse van Rensburg

A thesis submitted in partial fulfillment of the requirements for the degree of Master of Science in the Department of Molecular and Cell Biology, Faculty of Science, University of Cape Town, South Africa.

Cape Town

October 2007

Department of Molecular and Cell Biology, University of Cape Town,
Private Bag, Rondebosch, 7701, South Africa

TABLE OF CONTENTS

ABSTRACT

Although South Africa is the second largest producer of abalone outside Asia, the sustainability of the industry could be threatened by infectious diseases (Troell *et al.*, 2006). Probiotics are increasingly being viewed as an alternative to chemical and antibiotic treatments (Balcazar *et al.*, 2006), and have been shown to improve the health of the South African abalone, *Haliotis midae* (Macey and Coyne, 2005). In order to establish better health management systems, and to implement alternative therapies such as probiotics, a better understanding of how the abalone immune system functions, and specifically how it responds to stimulation, is necessary. Two genes of the electron transport system, cytochrome *b* and cytochrome *c* oxidase III, were found to be upregulated in a cDNA microarray experiment performed on haemocytes from immune-stimulated abalone (Arendze-Bailey, unpublished). The current study sought to confirm these results by semi-quantitative PCR and to further elucidate the roles of these genes, and thus the electron transport system, in the abalone immune response. This was done by specifically inhibiting cytochrome *b* with antimycin, and measuring haemocyte immune parameters *in vivo*. The expression of both cytochrome *b* and cytochrome *c* oxidase increased after immune stimulation which confirmed the results obtained from the microarray experiment. Phylogenetic analysis showed that both genes were closely related to the black lip abalone, *Haliotis rubra* as well as to other gastropods such as *Conus textile*. Antimycin did not decrease haemocyte cell viability, but halved cellular ATP from $4x10^{12}$ nM/cell to $2x10^{12}$ nM/cell. Inhibition of electron transport lead to a 0.6 fold increase in cellular superoxide levels, while phagocytosis dropped from 30% in control haemocytes to below 17% in treated samples. Though the antimycin seemed to reduce the bactericidal action of the haemocytes, the production of superoxide possibly interfered with the results obtained from the bactericidal assay, where antimycin was not found to significantly inhibit the killing of *E. coli* by haemocytes. Since both cytochrome *b* and cytochrome *c* oxidase III were upregulated in immune-stimulated abalone, and inhibition of electron transport lead to a decreased immune response *in vivo*, it was concluded that the immune response of the abalone is dependent on electron transport, and that oxidative phosphorylation plays a role in the immune response of abalone after stimulation.

CHAPTER 1

INTRODUCTION

CONTENTS

1.1 Abalone and Abalone Aquaculture

Abalone are herbivorous, marine molluscs and belong to the genus *Haliotis* (Stevens, 2003). Over 70 species of abalone have been found in the majority of the world's temperate oceans, occurring near the shore on rocky substrates, reefs and crevices (Stevens, 2003). Abalone is one of the most valuable seafood species in the world and its demand far exceeds supply (Reddy-Lopata *et al.*, 2006). Worldwide, fifteen species are commercially cultivated with over a thousand individual farms producing from less than a ton to over 200 metric tonnes (Gordon and Cook, 2001).

Natural abalone stocks have become depleted as a result of over 50 years of over-fishing, both for sport and commercial reasons, poaching, pollution of mainland habitat, disease and inadequate wild stock management (Stevens, 2003). As a result of the depletion of wild stocks, abalone farming began in the late 1950s and 1960s in Japan and China, and developed rapidly throughout the 1990s (Stevens, 2003). Between 1989 and 1999 wild abalone fisheries declined by approximately 30%, while global production increased by 600% (Stevens, 2003). Currently, abalone farming is widespread in many countries including the USA, Mexico, South Africa, Australia, Japan, China, Taiwan and Ireland (Stevens, 2003). By 2002, the global production of abalone reached 22 600 metric tonnes, with an estimated worth of US$ 0.8 billion (Troell *et al.*, 2006).

Since 1986, abalone fishing in South Africa has been regulated by minimum size, a restricted fishing season and a strict quota system (Troell *et al.*, 2006). Despite these measures, natural stocks still declined, mainly due to increased poaching (Troell *et al.*, 2006). Together with the overexploitation of wild stocks, high market prices were behind the development of the commercial abalone cultivation industry in South Africa (Troell *et al.*, 2006). Access to cheap labour, together with favourable coastal water quality and infrastructure also facilitated the rapid development of the industry in South Africa (Troell *et al.*, 2006). In 1996, the South African abalone aquaculture industry was deemed to be on the threshold of commercial production (Knauer *et al.*, 1996), and since then South Africa has become the largest producer of farmed abalone outside Asia (Troell *et al.*, 2006).

The present abalone fishery in South Africa is based on subtidal stocks of *Haliotis midae* (Troell *et al.*, 2006). This species is the only one of the six indigenous species that is commercially important (Reddy-Lopata *et al.*, 2006) and is distributed from Cape Columbine on the West Coast to the southern Transkei in the Eastern Cape Province (Troell *et al.*, 2006). Most of the abalone farms are located in the Western Cape Province, but others do exist as far as Port Nolloth in the Northern Cape Province and also in the Eastern Cape Province (Troell *et al.*, 2006).

Aquaculture of marine invertebrates is an economically important activity in many developing and developed countries, and infectious diseases are considered a major limitation to production in terms of quality, quantity, regularity and continuity of the industry (Mialhe *et al.*, 1995).

Numerous diseases have emerged as serious economic and ecological problems in aquaculture (Murray and Peeler, 2005). Viral, bacterial, rickettsial, chlamydial, protozoan and metazoan pathogens have been described in molluscs (Mialhe *et al.*, 1995). Due to poor food quality and high larval density in hatcheries, viral, bacterial and fungal infections are the most prevalent in larval production, while juveniles and adults are mostly affected by protozoan infections (Bachere, 2003). Aquaculture frequently results in high population densities which increase the risk of the establishment and spread of infection (Murray and Peeler, 2005).

Prevention and control of disease have led to an increase in the use of chemicals (Balcazar *et al.*, 2006) and treatment with antibiotics and chemotherapeutics continues to be important disease control methods in the aquaculture industry (Gram *et al.*, 2001). A range of chemicals is used in marine aquaculture, including disinfectants, antifoulants and antibiotics (Read and Fernandes, 2003). The environmental concerns over the use of these chemicals in the aquatic environment relate to the direct toxicity of the compounds to non-target organisms, the development of resistance to the compounds by pathogenic organisms, the prophylactic use of these chemicals, and the length of time they remain active in the marine environment (Read and Fernandes, 2003).

Chemical treatments may also lead to the destruction of the natural, non-pathogenic microbial community in the environment (Gomez-Gil *et al*, 2000), which is important for the development of a protective microbial community in the gut of the animals (Gomez-Gil *et al*, 2000). The gut community confers some measure of protection against infection, and when the environmental community is eliminated, this protective community cannot develop (Gomez-Gil *et al*, 2000). For this reason, the use of probiotics or beneficial bacteria, which control pathogens through a variety of mechanisms, is increasingly being viewed as an alternative to antibiotic or other chemical treatments (Balcazar *et al.*, 2006).

A probiotic is a bacterium which promotes the health of other organisms (Balcazar *et al.*, 2006). Probiotics beneficially affect the host animal by improving its microbial balance (Gomez-Gil *et al.*, 2000) and are usually isolated from indigenous and exogenous microbiota of aquatic animals (Balcazar *et al.*, 2006). Probiotics enhance colonization resistance in the host and have direct inhibitory effects against pathogens (Balcazar *et al.*, 2006). Some possible benefits linked to the administration of probiotics include: the competitive exclusion of pathogenic bacteria, the enhancement of enzymatic digestion, a source of nutrients and stimulation of the immune response against pathogenic microorganisms (Balcazar *et al.*, 2006). Work in our laboratory has shown that *Haliotis midae* fed a diet of probiotic-supplemented feed has a higher resistance to infection as well as an improved growth rate when compared to animals fed a diet of kelp (Macey and Coyne, 2005).

Due to uncontrolled poaching, the natural population of abalone in South Africa has declined drastically, leading to the rapid development of commercial abalone farming. Infectious diseases pose a threat to the abalone aquaculture industry, and in order to find methods to combat disease, more information regarding the immune response of the abalone needs to be obtained. Previous work in our laboratory has shown that feed supplemented with probiotics leads to an increased immune response in terms of phagocytosis and circulating haemocytes (Arendze-Bailey, unpublished, Macey, 2005), as well as the production of cellular reactive oxygen species (Macey, 2005). A cDNA microarray investigation of immune stimulated abalone haemocytes identified two electron transport chain genes, cytochrome *b* and cytochrome *c* oxidase III, to be differentially expressed in response to probiotic feeding (Arendze-Bailey, unpublished).

1.2 The Invertebrate Immune System

In order to establish health management systems in mollusc aquaculture, a better understanding of the effectors of the immune system and characterization of the defense response to infection and stress is necessary (Bachere, 2003). Current knowledge concerning the abalone immune system is based on limited work in abalone, variable amounts of work in other molluscs, some work in insects but mostly on work done in vertebrates (Hooper *et al.*, 2007).

Internal defense in invertebrate species is based on an innate, non-lymphoid immune system (Wootton and Pipe, 2003). Whereas vertebrates possess an acquired immune system with lymphocytes and immunoglobulins being major players, invertebrates do not posses immunoglobulins or memory following the first encounter with pathogens (Roch, 1999). The invertebrate immune system consists of a variety of cell types and effector molecules which interact to maintain efficient elimination of foreign bodies (Wootton and Pipe, 2003) including inorganic particles and living organisms, both pathogenic and non-pathogenic (Roch, 1999, Hooper *et al.*, 2007).

Immune function is largely effected by phagocytotic haemocytes and is complemented by an array of killing mechanisms, which may include the release of degradative and oxidative enzymes, the generation of highly reactive oxygen metabolites and the release of soluble compounds such as agglutinins, lectins and antibacterial peptides (Wootton and Pipe, 2003).

Haemocytes are divided into two main types: granulocytes and hyalinocytes (Cima *et al.*, 2000). Granulocytes form pseudopodia, can aggregate, show phagocytic activity, contain hydrolytic enzymes and peroxidases released via exocytosis (Cima *et al.*, 2000). Hyalinocytes are smaller than granulocytes and have a high nucleus:cytoplasm ratio (Cima *et al.*, 2000).

Phagocytosis, the main function of haemocytes, may be divided into well-defined stages, including recognition, chemotaxis, attachment, ingestion and destruction of foreign particles (Hooper *et al.*, 2007).

Discrimination of self from non-self is central to the immune function of all organisms, and in molluscs this occurs through opsonins or agglutinins, which are commonly known as lectins (Hooper *et al.*, 2007). Lectins are multimeric glycoprotein complexes that carry several sites for binding targets and are able to recognize and bind to non-self particles (Hooper *et al.*, 2007). After the lectin binds the target cell or particle, the lectin undergoes a conformational change, which exposes binding sites on the lectin, with which the haemocyte membrane receptors interact and so bind to the target cell or particle (Hooper *et al.*, 2007).

Chemotaxis is a process where haemocytes migrate towards and aggregate around invaders (Hooper *et al.*, 2007). Chemotaxis involves the directional migration of cells towards a chemo-attractant gradient, and this process is well understood in vertebrates and the same model is applied to studies in abalone (Hooper *et al.*, 2007).

Internalization involves the engulfment and encapsulation of foreign particles in a primary phagosome, which fuses with lysosomes to form a phagolysosome (Bachere *et al.*, 1995). Inside the phagolysosome, two main systems act to destroy, degrade and eliminate foreign particles – oxygen dependent systems (respiratory burst) and oxygen-independent systems.

Oxygen-independent systems include lysosomal enzymes, several of which have been identified in bivalve haemocytes, including acid phosphatase, lysozyme, b-glucuronidase, arylsuphatase, elastase, and cathepsin B and G (Bachere *et al.*, 1995, Hooper *et al.*, 2007). These enzymes act either intracellularly or extracellularly to digest foreign particles (Bachere *et al.*, 1995). Oxygen-independent defense also includes the release of antimicrobial peptides and serine proteases (Roch, 1999).

Phagocytosis is also associated with the respiratory burst which in bivalves is activated by foreign particles, organisms and their by-products and leads to the release of oxidants (Bugge *et al.*, 2007). During phagocytosis, increased amounts of oxygen are consumed, and the cell undergoes an oxidative or respiratory burst (Zelck *et al.*, 2005). The respiratory burst produces reactive oxygen species which act as killing agents, either alone or in combination with lysosomal enzymes, and are important for the elimination of viruses, bacteria, yeast, fungi and protozoa (Bugge *et al.*, 2007). These reactive oxygen species include superoxide anion,

hydrogen peroxide and other intermediate compounds with high bactericidal activity (Cima *et al.*, 2000) such as hydroxyl radicals and singlet molecular oxygen (Zelck *et al.*, 2005).

1.3 Mitochondria and the Electron Transport System

Animal cells derive energy from mitochondria through oxidative phosphorylation, a process in which electrons are passed along a series of carrier molecules called the electron transport chain (Watabe and Nakaki, 2007). These electrons are generated from NADH (reduced nicotinamide adenine dinucleotide) and succinates, which are produced by oxidation of nutrients such as glucose, and are ultimately transferred to molecular oxygen (Watabe and Nakaki, 2007).

Mitochondria are composed of four compartments (Sas *et al.*, 2007). The porous outer membrane encompasses the whole organelle and contains many important enzymes and receptors (Sas *et al.*, 2007). It is freely permeable to small molecules and ions. The convoluted inner membrane contains the enzymes responsible for oxidative phosphorylation, including the co-factor Q coenzyme, ubiquinone Q, ATP synthase and carrier proteins (Sas *et al.*, 2007). Between the two membranes is the intermembrane space which contains specialized proteins (Sas *et al.*, 2007). The matrix, which is bordered by the inner membrane, contains many enzymes involved in different metabolic pathways, including the citric acid cycle, fatty acid oxidation, and the urea cycle, and also mitochondrial DNA, peptidases and chaperones (Sas *et al.*, 2007). A diagrammatic representation of these compartments is shown in Figure 1.1.

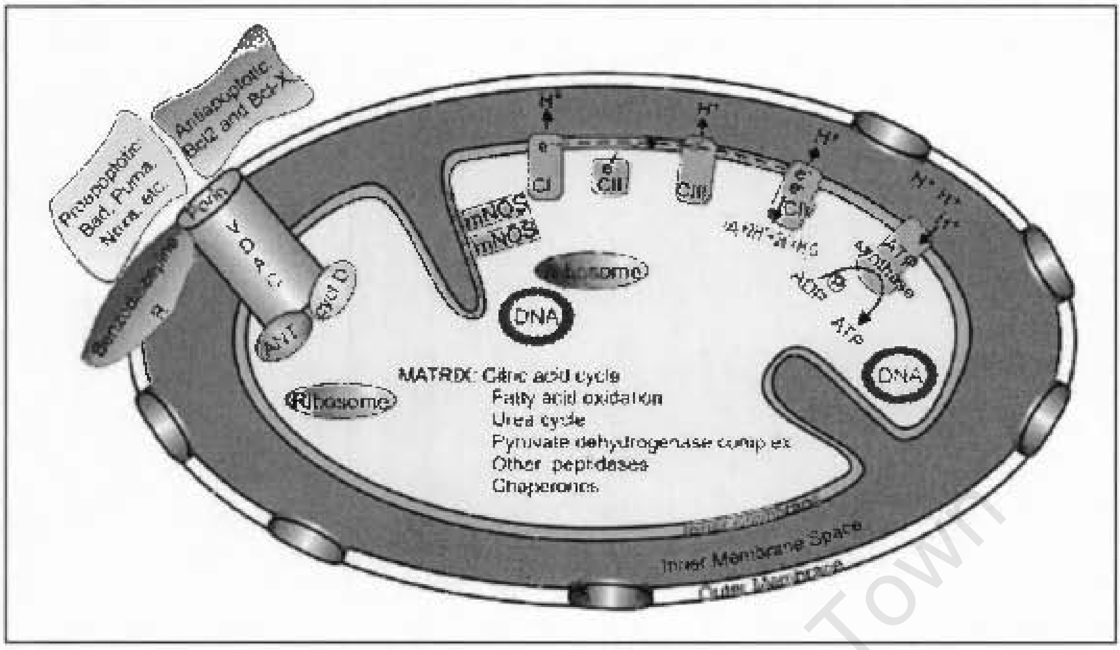

Figure 1.1 Structure of the mitochondrion (Sas *et al.*, 2007)

The mitochondrial electron transport chain consists of four respiratory complexes (I-IV). Complex I: NADH ubiquinone reductase; complex II: succinate ubiquinone reductase; complex III: ubiquinol cytochrome c reductase and complex IV: cytochrome c; while F_0F_1-ATP synthase is sometimes referred to as complex V (Sas *et al.*, 2007). The energy generated by the passage of electrons down the electron transport chain creates a proton gradient that drives ATP synthase to make ATP from ADP (Miyazaki *et al.*, 2003). The synthesized ATP is used for energy requiring reactions in the matrix, and is exported to the cytosol in exchange for cytosolic ADP (Miyazaki *et al.*, 2003).

Complex III is a homodimer and is also known as the *bc1* complex, or cytochrome *c* reductase (E.C. 1.10.2.2) (Matsuno-Yagi and Hatefi, 1999). During electron transfer from ubiquinol to cytochrome c, complex III is responsible for catalyzing proton translocation across the mitochondrial inner membrane (Bouzidi *et al.*, 1996). The enzyme has eleven subunits and the largest subunits, core proteins I and II, are important for the correct assembly of complex III. The next largest subunits, cytochromes *b* and *c1* and the Rieske iron-sulphur protein, are central catalytic units (Bouzidi *et al.*, 1996).

Cytochrome *b*, the only subunit of complex III that is encoded by the mitochondrial DNA, contains two heme groups and is the major transmembrane component of complex III (Bouzidi *et al.*, 1996). It is transcribed by polycistronic RNAs from the entire mitochondrial DNA, cut into precursor molecules and cleaved further into individual mRNAs that encode for both cytochrome *b* and NADPH-ubiquinone oxidoreductase subunit 5 (Kaminska *et al.*, 1997). Cytochrome *b* combines with nuclear encoded cytochrome *c1* to participate in the formation of complex III (Kaminska *et al.*, 1997).

Cytochrome *c* oxidase is the terminal enzyme of the electron transport chain, reducing oxygen to water, producing ATP through oxidative phosphorylation and so allowing energy and oxygen utilization by cells (Lienard *et al.*, 2006). Cytochrome *c* oxidase is located in the mitochondrial inner membrane where it transfers electrons from ferrocytochrome *c* to molecular oxygen (Barrientos *et al.*, 2002). The reaction is coupled to proton transfer from the matrix compartment to the intermembrane space, thereby contributing the energy stored in the electrochemical gradient to be used for ATP synthesis (Barrientos *et al.*, 2002).

Mitochondrial cytochrome *c* oxidase is made up of a variable number of subunits coded by the nuclear genome and three subunits (I, II and III) coded by the mitochondrial genome that constitute the catalytic core of the enzyme (Lienard *et al.*, 2006). Cytochrome *c* oxidase I contains the phosphorylation site while cytochrome *c* oxidase II interacts with cytochrome *c* during electron transfer (Lienard *et al.*, 2006). Cytochrome *c* oxidase III is involved in the transmembrane proton pumping mechanism as well as protecting cytochrome *c* oxidase active sites (Lienard *et al.*, 2006).

Cytochrome *c* oxidase III is a hydrophobic protein that spans the inner mitochondrial membrane. It is proposed to be involved in the folding, action and stability of cytochrome *c* oxidase (Khalimonchuk and Rodel, 2005). In the cytochrome oxidase homologue of *Rhodobacter sphaeroides*, cytochrome *c* oxidase III appears to be involved in maintaining rapid proton uptake, and limits enzyme turnover to prevent turnover induced inactivation (Khalimonchuk and Rodel, 2005). It is also thought to control back-leak of protons from the outer surface of subunit I (Hosler, 2004).

Mitochondria consume 90% of the oxygen used by the cell and although there are a number of different cellular sources of reactive oxygen species, the electron transport chain is a major source of reactive oxygen species (Sandeep *et al.*, 2000) as it is responsible for generating a continuous flux of oxygen radicals (Petrosillo *et al.*, 2003). It is estimated that 1-2% of all electrons passing through the respiratory chain end up as oxygen radicals (Sandeep *et al.*, 2000), with unpaired electrons escaping mainly from complex I and III (Sas *et al.*, 2007).

The formation of superoxide occurs via the transfer of a free electron to molecular oxygen and this reaction occurs at specific sites of the electron transport chain (Petrosillo *et al.*, 2003). Free electrons may react non-enzymatically with oxygen, forming superoxide anion radicals and converted enzymatically or spontaneously to other reactive oxygen species (Vrbacky *et al.*, 2007). Although reactive oxygen species are produced from both complex I and III, ubiquinone from complex III is considered to be a major source of superoxide anion generation in the mitochondria (Petrosillo *et al.*, 2003).

1.4 Antimycin

A property that characterizes mitochondrial respiration is its sensitivity towards antimycin (Rieske *et al.*, 1967). Inhibition of the electron transport chain causes a collapse of the proton gradient across the inner mitochondrial membrane, thereby collapsing the mitochondrial membrane potential which eventually leads to cell death through apoptosis (Park *et al.*, 2007). Antimycin is used to investigate mitochondrial reactive oxygen species generation and to model or simulate hypoxia (Zhang *et al.*, 2001). Antimycin is a fungicidal agent that inhibits the growth of molds and yeasts in low concentrations, and is bactericidal in very high amounts (Marquis, 1965). It is also a respiratory inhibitor in mammals and higher plants (Marquis, 1965). Antimycin is a mixture of antimycin A1 and A3 from *Streptomyces kitazawensis* (Park *et al.*, 2007). It inhibits succinate oxidase and NADH oxidase and also inhibits mitochondrial electron transport between cytochrome *b* and *c1* (Park *et al.*, 2007) by blocking electron flow in the Q-cycle of complex III. Antimycin also enhances the transfer of single electrons to molecular oxygen, producing superoxide (Meany *et al.*, 2006).

1.5 Measuring Invertebrate Immune Function

Various methods for measuring of the ability of bivalve haemocytes to generate a defense response against pathogenic and other non-self particles have been developed (Volety *et al.*, 1999). These methods include measurement of cellular responses such as phagocytosis and superoxide production, as well as humoral responses such as the release of acid phosphatase or non-specific esterases (Wootton *et al.*, 2003).

Phagocytosis is important in the elimination of microorganisms or foreign particles (Roch, 1999) and the phagocytosis assay is used to measure the proportion of ingested particles or the proportion of haemocytes that have ingested labeled particles (Hooper *et al.*, 2007). These particles may be fluorescently labeled bacteria (Ohta *et al.*, 2006) or fluorescent beads (Ling and Yu, 2006). The use of flow cytometry to measure phagocytosis in haemocytes has also been described (Brousseau *et al.*, 2000).

The respiratory burst, which occurs concomitantly with phagocytosis, may be measured by means of fluoroprobes (Mukhopadhyay *et al.*, 2007), chemiluminescence (Fossati *et al.*, 2003), flow cytometry (Bugge *et al.*, 2007), or the reduction of nitroblue tetrazolium (NBT) to a purple formazan (Soria *et al.*, 2006), where the absorbance of the formazan is proportional to the amount of superoxide formed.

While most immune assays reflect only one facet of the haemocyte response, quantification of pathogen viability following exposure to hemocytes provides a comprehensive representation of immunocompetence by integrating the sequential activities of recognition, locomotion, phagocytosis and degradation (Volety *et al.*, 1999). A variety of techniques have been used to quantify the viability of cells from various organisms (Volety *et al.*, 1999). These techniques include enumeration of cells that either include or exclude dyes, incorporate radiolabelled nucleotides, grow on agar or reduce tetrazolium dyes (Volety *et al.*, 1999). Dye reduction methods offer simplicity, rapidity, reproducibility and potential for automation (Volety *et al.*, 1999).

1.6 Aims of the Study

The aim of this study was firstly to confirm the identity and putative function of the genes. Furthermore, the study aimed to confirm that both genes are indeed upregulated by immune-stimulation, by studying their expression after probiotic feeding using semi-quantitative PCR.

A second part of the study was to determine what the role of these genes and their protein products, which form part of oxidative phosphorylation, are in the immune response of the abalone. As the genes code for components of specific respiratory complexes, they do not act alone, but rather as part of electron transport as a whole. Therefore, the role of electron transport during the immune response of the abalone, as well as the dependency of the immune response on electron transport was investigated. This was done by specifically inhibiting cytochrome *b* with antimycin, and then measuring specific haemocyte immune parameters *in vitro*. In this case, electron transport isn't viewed as an effector of defense but merely as an indicator of cellular activity.

To ensure that any decrease in immune response was due to inhibition of the electron transport chain and not because antimycin has a negative effect on the viability of the haemocytes, an MTT assay was used to check that the concentration of antimycin used, as well as the incubation time, did not decrease haemocyte viability. Following this, a luciferin/luciferase ATP assay was used to measure the end-product of the electron transport chain, ATP, to ensure that electron transport was indeed being inhibited.

A phagocytosis assay was used to determine what effect antimycin has on this aspect of the immune response. If antimycin did lead to a decrease in phagocytosis, it would mean that this process was reliant on oxidative phosphorylation. Furthermore, the role of electron transport during the destruction of pathogens was investigated using a bacterial killing assay. This assay measured the ability of bacteria to proliferate in growth media after being exposed to haemocytes using an MTT assay. If the proliferation of bacteria decreased after exposure to haemocytes, it would mean that the killing mechanisms of the haemocytes were active and functional.

Treatment with antimycin would determine whether this function of the immune response was dependent on oxidative phosphorylation.

The production of superoxide anion due to antimycin binding to cytochrome *b* and blocking electron flow was investigated. If antimycin led to increased amounts of cellular reactive oxygen species, the implication of the increased reactive oxygen species on other immune functions such as pathogen killing would have to be considered, as well as the effect that the oxidants were having on the viability of the haemocytes, and whether this in turn was affecting the normal function of the immune response.

In order to effectively manage diseases in abalone aquaculture, it is necessary to have a full understanding of the effectors of their immune system and as well as the mechanisms of defense against diseases (Bachere, 2003). For this reason, an understanding of the genes involved in the immune response, as well as the roles of the pathways they form part of is important. The results from this study will assist in furthering our knowledge of the abalone immune system, as well as the role that the electron transport chain plays in defense against invading pathogens. It will also give insight into how probiotic-feeding stimulates the abalone immune response, which in turn will give insight into the great potential that probiotics have as a natural method of disease control in cultured abalone.

CHAPTER 2

MATERIALS AND METHODS

CONTENTS

2.1 Confirmation of microarray

The abalone immune response has been shown to be maximally stimulated 18 hours after feeding a probiotic-supplemented feed (Arendze-Bailey, unpublished). Both cytochrome *b* and cytochrome *c* oxidase III were identified to be upregulated in a cDNA microarray experiment conducted on immune-stimulated abalone (Arendze-Bailey, unpublished). The aim of this experiment was to confirm the data from the microarray, using semi-quantitative PCR.

2.1.1 Animals

Abalone were maintained at the Marine and Coastal Management Research Aquarium in Sea Point, Cape Town, South Africa. The animals were maintained in 98 l polyethylene tanks containing aerated and continuously flowing natural seawater between 17 and 18 °C. The tanks contained two baskets each, and were stocked with 80 abalone (40 animals/basket). Between experiments, the abalone were fed kelp twice a week.

2.1.2 Collection of haemolymph

Haemolymph, approximately 500 µl/animal, was collected from the pedal sinus using 1.5 ml syringes and 26 G ½ inch needles and pooled to obtain desired volume for experiment. The haemolymph was kept on ice during transport from the aquarium to the laboratory (approximately 30 min).

2.1.3 Total Haemocyte Count

The number of haemocytes/ml was determined directly after collection. Undiluted haemolymph (100 µl) was added to 200 µl Alsever's Buffer (Appendix A.2.1). The number of cells was counted using a haemocytometer and a light microscope at 100x magnification. Haemocyte concentration was calculated using the following equation:

Haemocyte concentration = [(Cell count/0.1)/0.16] x 1000 x 3 = cells/ml

2.1.4 Preparation of the probiotic feed

Vibrio midae SY9, isolated by Macey (2005) was grown in 5 ml marine broth (Appendix A.1.1) at room temperature with shaking for 12 hours. Subsequently, 500 µl of culture was transferred to 50 ml of fresh media and incubated for a further 12 hours. Following this, 500 ml of fresh media was inoculated with a volume equivalent to an absorbance value of 0.01 at 600 nm. The cultures were incubated overnight where after they were washed twice in PBS (Appendix A.2.3), and resuspended in approximately 20 ml of PBS.

Cryptococcus strain SS1 and *Debaryomyces hansenii* AY1, isolated by Macey (2005) were grown in 5 ml yeast tryptone broth (Appendix A.1.2) at room temperature with shaking for 24 hours. Subsequently, 500 µl of culture was transferred to 50 ml of fresh media and incubated for a further 24 hours. Following this, 500 ml of fresh media was inoculated with a volume equivalent to an absorbance value of 0.01 at 600 nm. The cultures were incubated for a further 24 hours, washed twice in PBS and resuspended in approximately 20 ml of PBS.

To prepare the probiotic-supplemented feed, kelp cakes were prepared as described in Appendix A.1.4, with an equal volume of each of the three resuspended probiotic cultures added to the kelp cake mix. The probiotic-supplemented feed was stored at 4 °C until used for up to a week.

2.1.5 Experimental Setup

A week before the experiment, all of the abalone were fed a diet of kelp cakes, without probiotics, with each basket receiving two kelp cakes twice a week. The abalone in the first tank (tank A) would serve as control animals, while the abalone in the second tank (tank B) would be immune-stimulated through the probiotic-supplemented feed (Figure 2.1).

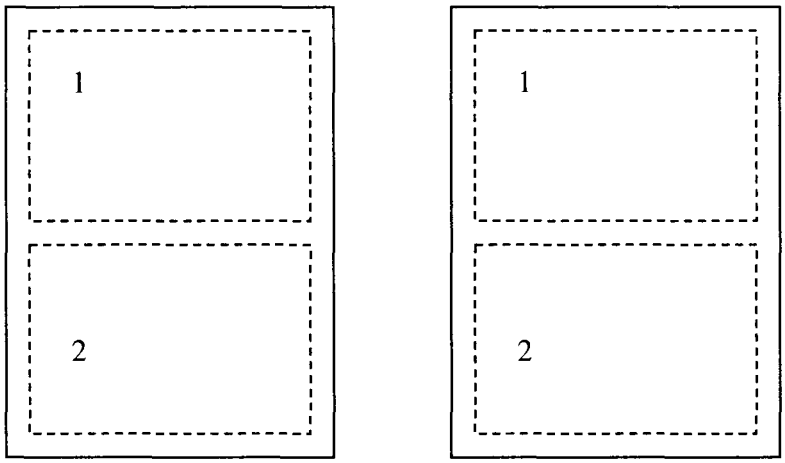

Tank A – Control feed Tank B – Probiotic feed

Figure 2.1. Diagrammatic representation of the experimental setup. Each tank contained a total of 80 animals (40 abalone/basket). The animals in tank A were fed a diet of kelp cakes, while the animals in tank B were given the probiotic-supplemented kelp cakes.

At the beginning of the experiment (time point 0), the abalone in tank A (control animals) were fed regular kelp cakes, two kelp cakes per basket, while the abalone in tank B (immune-stimulated animals) were fed the probiotic-supplemented kelp cakes, also two per basket. All of the animals were fed again after 12 and 24 hours, two kelp cakes per basket. Blood was drawn from four animals from each tank at 0, 6, 12, 18, 24, 36, and 48 hours. Animals from which blood was drawn were moved to a separate holding tank in order to avoid sampling from the same animals. Aliquots of undiluted haemolymph were prepared for cell counting as described in 2.1.3. Undiluted haemolymph (800 µl) was added to 200 µl anti-coagulation buffer (Appendix A.6.2). Unless used immediately, the samples were flash frozen in liquid nitrogen and stored at -70°C.

2.1.6 RNA Isolation

Samples, collected as described in section 2.1.5, were thawed on ice and centrifuged for 5 minutes at 3000 x *g* at 4 °C. The haemocytes were resuspended in 500 µl lysis solution (Appendix A.6.3) using a 1 ml syringe and 21 G ½ inch needle.

Samples were transferred to 2ml eppendorf tube and homogenized by adding approximately 0.5 volume acid washed glass beads and vortexing for 1 minute. After adding 50 µl 2 M sodium acetate pH 4 (Appendix A.6.4) and 500 µl phenol pH 5, 100 µl chloroform:isoamyl alcohol (49:1) was added and incubated on ice for 15 minutes. Separation of the aqueous phase was achieved by centrifugation for 20 minutes at 3000 x *g* at 4 °C. The aqueous phase was removed and incubated with 1 volume isopropanol at – 70 °C overnight to precipitate the RNA.

After the RNA had precipitated, the samples were centrifuged at 3000 x *g* for 20 minutes at 4 °C. The RNA was resuspended in 100 µl lysis solution (Appendix A.6.3) and incubated at – 20 °C for 1 hour.

Precipitated RNA was centrifuged at 3000 x *g* for 10 minutes at 4 °C. The supernatant was discarded and the pellet washed with ice cold 96 % ethanol followed by 75 % ethanol. The RNA pellet was dried and resuspended in 50 µl DEPC-dH_2O (Appendix A.6.1)

RNA was quantitated on a Nanodrop® ND-1000 UV-Vis Spectrophotometer (Nanodrop Technologies) and the integrity checked on a denaturing agarose gel (Appendix A.3.3). Samples were diluted 1:2 in sample buffer (Appendix A.3.4), heated to 65 °C for 5 min and snap cooled on ice prior to loading on the gel. RNA was stored at – 70 °C until used.

2.1.7 RT-PCR

Conversion of RNA to cDNA was performed using the ImProm-II™ Reverse Transcription System (Promega) and the conditions as described in Appendix C.3.

2.1.8 DNA Isolation

Undiluted haemolymph (1 ml), collected as described in section 2.1.2, was centrifuged for 5 minutes at 3000 x *g*. The serum was discarded and the haemocytes washed in 1 ml ice-cold PBS. The haemocytes were resuspended in an extraction buffer containing 567 µl Tris/EDTA Buffer (Appendix A.5.1), 30 µl 10% SDS and 3 µl Proteinase K (Sigma). After incubation at 37 °C in a

thermoregulated waterbath for 1 hour 100 µl of 5 M NaCl (Appendix A.5.2) and 80 µl of CTAB/NaCl (Appendix A.5.3) was added and incubated at 65 °C for 10 minutes. An equal volume of chloroform:isoamyl alcohol (24:1) was added and the samples centrifuged for 5 minutes at 3000 x *g*. The aqueous phase was removed, 0.6 volumes isopropanol added and the sample centrifuged for 15 minutes at 3000 x *g*. The supernatant was discarded and the pellet washed in 70% ethanol. After air drying, the pellet was resuspended in 50 µl Tris/EDTA buffer supplemented with 1 µl of 10 mg/ml RNase A (Sigma).

The DNA was quantitated on a Nanodrop ND-1000 and the integrity of the DNA checked on a 0.8 % agarose gel prepared in TAE containing 10 µg/ml ethidium bromide (Sigma).

2.1.9 Plasmid Isolation

Plasmid isolation was performed according to the alkaline lysis method as described by Sambrook (1989). A 5 ml overnight culture of *E. coli* DH5α was prepared by growing bacteria in Luria broth (Appendix A.1.3) supplemented with either chloramphenicol (30 mg/ml, Appendix A.4.1), for transformants containing the pDNR-LIB vector (Appendix B.1, CLONTECH Laboratories, Inc), or ampicillin (10 mg/ml Appendix A.4.1) for transformants containing the pGEM-T Easy vector (Appendix B.2, Promega), at 37°C.

A 2 ml aliquot of the 5 ml overnight culture was transferred to a 2 ml eppendorf tube, centrifuged for 30 s at 3000 x *g* and the supernatant removed. An additional 2 ml of culture was added to the pellet, and centrifuged again. The cell pellet was then resuspended in 0.2 ml Solution 1 (Appendix A.4.2) and left at room temperature for 10 min to allow for cell lysis. Following this 0.4 ml Solution 2 (Appendix A.4.3) was added and the cell mixture was left to incubate on ice for 10 min. Pre–cooled Solution 3 (Appendix A.4.4) was then added to precipitate chromosomal DNA, and the cell mixture was left on ice for 10 min. Plasmid DNA was recovered through centrifugation at room temperature for 5 min. The supernatant containing the plasmid DNA was transferred to a fresh tube to which 0.6 ml isopropanol was added. The mixture was left for 2 min at room temperature and centrifuged at 3000 x *g* for 10 min. The pellet was retained and washed in 70 % ethanol by inversion, air-dried and re-dissolved in 30 µl

sterile dH_2O.

2.1.10 Primer design

Primer pairs for the amplification of the cDNA microarray clones putatively identified as cytochrome *b* and cytochrome *c* oxidase III by Arendze-Bailey (unpublished) were designed using FastPCR (©1999-2006, University of Helsinki). FastPCR automatically identifies optimal primers for PCR using the following parameters: the general nucleotide structure of the primer such as complexity, nucleotide composition at the 3' and 5' ends, the melting temperature of the 10 bases at the 3' and 5' ends, self-complementarity and secondary (non-specific) binding. The melting temperature is calculated using a formula based on nearest neighbour thermodynamic theory with unified dS, dH and dG parameters (Allawi and Santa-Lucia, 1997) and the optimal annealing temperature is calculated by the formula of Rychlik *et al.* (1990). A primer pair for amplification of the *H. midae* actin gene, which had been previously cloned and sequenced in our lab, was also designed using FastPCR. The sequences for all the primer pairs are shown in Appendix C.1.

2.1.11 Polymerase Chain Reaction (PCR)

To determine whether cytochrome *c* oxidase III and cytochrome *b* could be amplified directly from genomic DNA, PCR was carried out in a Bioer XP Thermal Cycler (Bioer Techology Co.). PCR reactions were carried out using 1 x PCR buffer, 2 mM $MgCl_2$, 0.4 µM dNTPs, 0.5 µM of each primer, 1 U Taq polymerase and 300 ng genomic DNA template and cycling conditions as described in Appendix C.2. The clones from the cDNA library were used as positive controls. The reaction conditions were the same as those employed to amplify the genomic DNA, except that 5 ng of plasmid DNA template was used.

2.1.12 Semi-Quantitative PCR

PCR reactions were carried out in a Bioer XP Thermal Cycler (Bioer Techology Co.) using 1 x PCR buffer, 2.5 mM $MgCl_2$, 0.4 mM dNTPs (Promega), 0.5 µM of each primer, 1 U Super-

Therm Taq polymerase (Southern Cross Biotechnology), and 1 µl cDNA template in a final volume of 25 µl. The number of amplification cycles used for each primer set is described in Appendix C.2

After amplification, the PCR product was analysed on a 3% agarose gel prepared in TAE (Appendix A.3.1) followed by densitometric analysis, which was conducted as follows:

An image of each gel was captured using the UV light of a Biorad GelDoc EQ-system™ (Biorad Laboratories), using the same exposure time, roughly 0.5 seconds, for each gel. Image processing and analysis was carried out using Quantity-One software (© 2004 Biorad Laboratories). None of the optimization affected the underlying data; it merely enhanced the image display to aid in the analysis of the data. Firstly, the images were transformed to adjust the brightness and contrast of the images. This was done using an auto scale option which optimizes the image automatically; it enhances minor variations in the image and makes fine details easier to see. Next, image background due to gel opacity was removed using an automatic whole background subtract function. The image was filtered, which removes small noise features while leaving larger features such as DNA bands unaffected. Finally, the boundary of each band was defined, and the total signal intensity within that boundary measured by generating a density analysis report. This function reports the density of a band as the total intensity of all the pixels included in the defined boundary divided by the area of the defined boundary.

The density of the PCR product at each time point was divided by the density of the time 0 sample, and therefore, the fold change in gene expression in immune-stimulated samples is reported as a function of gene expression at time 0.

2.1.12.1. Optimization of PCR conditions for semi-quantitative PCR

For semi-quantitative analysis the PCR must be in the exponential range during which the amplified products double with each cycle. To define the exponential range, several PCRs were

performed where the reaction was stopped after every 5 cycles. The PCR products were loaded on a 5% agarose gel prepared in TAE and the relative increase in PCR products evaluated.

2.2 Sequence analysis

Preliminary analysis of the nucleotide sequences of two cDNA clones identified by microarray analysis as upregulated in immune-stimulated abalone identified them as cytochrome *b* and cytochrome *c* oxidase III respectively (Arendze-Bailey, unpublished). Preliminary sequence of the cDNA clone identified as cytochrome *c* oxidase III showed that it did not include a complete open reading frame, and therefore 5' Rapid Amplification of cDNA Ends (RACE) was employed to obtain the full length sequence of cytochrome *c* oxidase III.

2.2.1 5' RACE of cytochrome *c* oxidase III

5'RACE of cytochrome *c* oxidase III was performed using the SMART™ RACE cDNA Amplification Kit (Clontech Laboratories, Inc.) according to the manufacturer's instructions. A gene specific primer (Appendix C.1.4) was designed based on the known sequence using FastPCR according to the prerequisites as described for the kit and PCR was carried out using the cycling conditions stipulated in Appendix C.2.4. The amplified product was cloned into the pGEM-T® Easy Vector system (Promega) according to the manufacturer's instructions and transformed into *E. coli* DH5α cells. Plasmid DNA was isolated using the method described in section 2.1.9. and sequenced using universal M13F and M13R primers (Appendix C.1.5). Sequencing reactions and electrophoresis were performed by Macrogen Inc. (Seoul, South-Korea).

2.2.2 Sequence and phylogenetic analysis

2.2.2.1 Cytochrome *b*

A BLASTX search, using the sequence from the cDNA library clone, was conducted against the database of protein sequences provided by the National Centre for Biotechnology Information (NCBI) internet site (http://www.ncbi.blast.nlm.nih.gov/BLAST/). The ORF-finder function, also provided by the NCBI (http://www.ncbi.nlm.nih.gov/gorf/gorf.html) was used to identify possible open reading frames and to predict a putative amino acid sequence. Using the Conserved Domain Search function also provided by the NCBI (http://www.ncbi.nlm.nih.gov/Structure/cdd/wrpsb.cgi), possible conserved domains within the putative amino acid sequence were identified.

The putative amino acid sequence of the cytochrome *b* cDNA library clone was aligned with 26 known cytochrome *b* protein sequences obtained from the NCBI protein database. Species and accession numbers were: *Homo sapiens* (NP_536855.1), *Pan troglodytes* (NP_008198.1), *Canis lupus familiaris* (NP_008483.1), *Mus musculus* (NP_904340.1), *Rattus norvegicus* (YP_665641.1), *Gallus gallus* (NP_006926.1), *Danio rerio* (NP_059343.1), *Drosophila melanogaster* (NP_008288.1), *Anopheles gambiae* (NP_008080.1), *Caenorhabditis elegans* (NP_006958.1), *Graptacme eborea* (YP_073350.1), *Argopecten irradians* (YP_001382291.1), *Placopecten magellanicus* (YP_272043.1), *Mytilus edulis* (YP_073336.1), *Todarodes pacificus* (YP_112461.1), *Octopus vulgaris* (YP_112443.1), *Argulus americanus* (YP_026006.1), *Penaeus monodon* (NP_038299.1), *Haliotis rubra* (YP_026076.1), *Conus textile* (YP_001004254.1), *Phlebotomus perniciosus* (AAD44996.1), *Fenneropenaeus chinensis* (ABG65676.1), *Litopenaeus vannamei* (YP_001315043.1), *Daphnia pulex* (ABD19355.1), *Acheta domesticus* (AF248682_1), *Halocaridina rubra* (YP_778666.1), *Squilla mantis* (YP_054555.1) The sequences were aligned using the optimal alignment option of CLUSTAL X version 1.83 (Thompson *et al.*, 1997). Alignments were exported in clustal format for phylogenetic and molecular evolutionary analysis using MEGA version 3.1 (Kumar and Nei, 2004). A Neighbour Joining (NJ) (Saito and Nei, 1987) tree was constructed from the data set using MEGA. The

reliability of the inferred phylogenetic trees was assessed using the bootstrap test (Felsenstein, 1985). Five hundred replicates were tested with a random starting seed.

2.2.2.2 Cytochrome *c* oxidase III

The sequence of the cDNA library clone and that obtained with 5' RACE was assembled using DNAMan v 4.1.3 (Lynnon Biosoft© 1994-1999). A BLASTX search, using the assembled sequence, was conducted against the database of protein sequences provided by the National Centre for Biotechnology Information (NCBI) internet site (http://www.ncbi.blast.nlm.nih.gov/BLAST/). The ORF-finder function, also provided by the NCBI (http://www.ncbi.nlm.nih.gov/gorf/gorf.html), was used to identify possible open reading frames and to predict a putative amino acid sequence. Using the Conserved Domain Search function (http://www.ncbi.nlm.nih.gov/Structure/cdd/wrpsb.cgi), possible conserved domains within the putative amino acid sequence were identified.

The putative amino acid sequence of cytochrome c oxidase III was aligned with 22 known cytochrome *c* oxidase III protein sequences obtained from the NCBI protein database. The sequence and accession numbers were: *Homo sapiens* (NP_536849.1), *Pan troglodytes* (NP_008192.1), *Canis lupus familiaris* (NP_008477.4), *Mus musculus* (NP_904334.1), *Rattus norvegicus* (YP_665635.1), *Gallus gallus* (NP_006921.1), *Danio rerio* (NP_059337.1), *Drosophila melanogaster* (NP_008282.1), *Anopheles gambiae* (NP_008074.1), *Argulus americanus* (YP_026012.1), *Penaeus monodon* (NP_038293.1), *Daphnia pulex* (AAB53201.1), *Haliotis rubra* (YP_026066.1), *Conus textile* (YP_001004258.1), *Sepia officinalis* (YP_514793.1), *Artemia franciscana* (NP_007113.1), *Squilla mantis* (YP_054549.1), *Triops longicaudatus* (YP_054523.1), *Litopenaeus vannamei* (YP_001315037.1), *Halocaridina rubra* (YP_778660.1), *Ostrinia furnacalis* (NP_563601.1), *Bombyx mori* (BAB84666.1)

The sequences were aligned using the optimal alignment option of CLUSTAL X version 1.83 (Thompson *et al.*, 1997). Alignments were exported in clustal format for phylogenetic and molecular evolutionary analysis using MEGA version 3.1 (Kumar and Nei, 2004). A Neighbour Joining (NJ) (Saitou and Nei, 1987) tree was constructed from the data set using MEGA. The

reliability of the inferred phylogenetic trees was assessed using the bootstrap test (Felsenstein, 1985). Five hundred replicates were tested with a random starting seed.

2.3 The role of cytochrome *c* oxidase III and cytochrome *b* in the immune response of *Haliotis midae*

The role of the two genes in the immune response of the abalone was studied *in vitro* using antimycin, which is an inhibitor which specifically blocks transport of electrons between cytochrome *b* and cytochrome *c*.

2.3.1 Attachment of abalone haemocyte monolayers

After haemolymph collection (2.1.2), 100 µl haemolymph was placed into each well of a 96-well microtitre plate and adjusted to a cell density of 2 x 10^8 cells/ml per well and allowed to attach for 20 min at room temperature in a humidified chamber. After attachment, the serum was removed, the haemocytes washed with PBS and kept in 100 µl MHBSS (Appendix A.2.2) until the assays were performed. Monolayers were prepared for each experiment as needed.

2.3.2 Treatment of haemocyte monolayers with antimycin

A stock solution of antimycin (Sigma) was prepared in 100% ethanol (100 mg/ml, final concentration) and diluted to the desired concentration in PBS. After incubation with antimycin for the required time, the antimycin was removed and the haemocyte monolayers washed in PBS and the chosen assay performed.

2.3.3 ATP assay to measure the effect of antimcyin on electron transport

Since ATP is the final product of the electron transport chain, a decrease in ATP indicates that antimycin is inhibiting haemocyte respiration. ATP levels in the haemocytes were measured using an ATP Determination Kit (Invitrogen Molecular Probes) which is based on a

luciferin/luciferase reaction. A Standard Reaction Solution, containing water, 20X reaction buffer, 0.1 M DTT, 10 mM D-luciferin and 2.5 µl of 5 mg/ml firefly luciferase was prepared according to the manufacturers' instructions. Haemocyte monolayers were treated for 2 hours with PBS in the case of the control samples, and 100 µl of 100 µM antimycin for the test samples. Haemocytes were harvested by incubation in 100 µl of 10 mM EDTA (Appendix A.8.2) for 10 min. A 10 µl sample of the detached cells was removed for cell number determination (Section 2.1.3) in order to correct for cells lost during detachment. The remaining sample was centrifuged for 5 min at 3000 x g. The supernatant was removed and the pellet resuspended in cell lysis buffer (Appendix A.8.1). After incubating for 15 minutes on ice, the samples were centrifuged again and 10 µl of the supernatant was added to 100 µl of Standard Reaction Solution and incubated for 20 minutes at room temperature in the dark to ensure that the luminescent signal was stable. Following this, the relative luminescence was measured in a TD 20/20 luminometer (Turner Designs).

A standard curve was constructed each time the experiment was performed. Low-concentration ATP standard solutions were prepared by diluting the standard ATP solution (5 mM) provided with the kit in dH_2O. The concentration of the standards ranged from 5 mM to 5 pM. To 100 µl of Standard Reaction Solution, 10 µl of each of these standards was added, and after incubating for 20 minutes in the dark, the luminescence was measured. Using the values obtained on the standard curve, the luminescent readings of the samples could be converted to concentration of ATP. Because the number of cells per sample was also determined using a haemocytometer, the ATP per sample could be expressed as nM of ATP/cell.

2.3.4 MTT (3-(4, 5-Dimethylthiazol-2-yl)-2, 5-diphenyltetrazolium bromide) assay to measure the effect of antimycin on haemocyte viability

Because antimycin inhibits electron transport, it might have a negative effect on the viability of the haemocytes, which might lead to a diminished immune response. To ensure that any decrease in the immune response was directly caused by inhibition of electron transport and not as a consequence of non-viable haemocytes, an MTT assay was performed on haemocytes treated with 1 µM, 10 µM and 100 µM antimycin for two hours. Also included in this

experiment were samples treated with the equivalent amount of ethanol that the antimycin was dissolved in, to ensure that the ethanol did not have a negative effect on haemocyte viability.

After incubation with antimycin, the supernatant was removed and the haemocytes rinsed with PBS. The haemocyte monolayers were incubated with 20 µl MHBSS and 20 µl MTT (5 mg/ml, Sigma) for 3 hours. After incubation, the supernatant was removed and the haemocytes rinsed twice with MHBSS. Solubilization of the purple precipitated formazan was achieved by adding 100 µl acidic isopropanol (Appendix A.7.1) and incubation of the samples overnight on a plate shaker. Quantification of the formazan product was performed spectrophotometrically at 540 nm using a Nanodrop® ND-1000 UV-Vis Spectrophotometer, where the absorbance at 540 nm represents the ability of haemocyte mitochondrial enzymes to reduce MTT, and is therefore a measure of the viability of the haemocytes.

2.3.5 NBT (Nitroblue Tetrazolium) assay to measure the effect of antimycin on the production of cellular superoxide anion

This assay, as described by Malham *et al.,* (2003) and modified by Macey (2005) was performed to determine whether treatment with antimycin causes an increase in cellular superoxide anion production. A stock stolution of NBT (10 mg/ml, Sigma) was prepared in dH_2O, and from this a working solution of 2 mg/ml was prepared in PBS. Haemocyte monolayers were incubated with 100 µl NBT and either PBS (control samples) or 100 µl 100 µM antimcyin (test samples). Additional negative controls, such as superoxide dismutase (SOD), were omitted as they had been performed by Macey (2005) who showed that the reaction was specific. The samples were incubated in the dark for 2 hours, whereafter the supernatant was removed and the haemocytes fixed by incubating with 100 µl 100 % methanol for 10 minutes. The supernatant was removed, the cells were air dried and the precipitated formazan was dissolved by adding 120 µl 2 M KOH (Appendix A.9.1) and 140 µl DMSO. The absorbance was determined at 620 nm on a Nanodrop® ND-1000 UV-Vis Spectrophotometer. As NBT is reduced by superoxide anion, the absorbance can be directly related back to the amount of superoxide anion present inside the haemocytes.

2.3.6 Phagocytosis assay to measure the effect of antimycin on the removal of pathogenic bacteria

To determine whether inhibition of the electron transport system would have an effect on the recognition and phagocytosis of pathogens, phagocytosis assays were performed comparing haemocytes incubated for 2 hours in either PBS or antimycin.

The phagocytosis assay was performed as described by Malham *et al,* (2003) and Macey and Coyne (2005). *Vibrio anguillarum* was grown at room temperature overnight in TSB (Biolab) supplemented with 2.5% (w/v) NaCl. After killing the bacteria by the addition of 10% formalin, the cells were centrifuged at 12 000 x *g* for 10 min. The cells were washed twice in PBS and resuspended in 0.1 M $NaHCO_3$ pH 9.0 (Appendix A.10.1) containing 0.1 mg/ml fluorescein 5-isothiocyanate, isomer 1 (FITC, Sigma). Cells were labeled by incubation at room temperature for 1 hour in the dark. Unincorporated FITC was removed by centrifugation and the bacteria resuspended in PBS. The bacteria were diluted to 10^8 cells/ml and stored at -20 °C until used.

Haemolymph (100 µl) containing 10^6 cells/ml in MHBSS was placed inside a silicon ring on a glass slide, and incubated for 20 min in a dark moist chamber. Unattached haemocytes were removed by washing twice with MHBSS. FITC-labeled bacteria (100 µl) were added to the monolayer and incubated for 30 min in a dark moist chamber. The slides were washed twice with MHBSS and fixed by washing once with methanol. The haemocytes were stained with 100 µl ethidium bromide (1 mg/ml, Appendix A.10.2) for 1 minute. After rinsing twice with MHBSS, excess moisture was removed and coverslips placed on the silicon ring. Phagocytic cells were distinguished from non-phagocytic cells by the fact that they contained green fluorescent bacteria. Percentage phagocytosis was determined by counting two hundred cells per slide in triplicate using a 488 nm emission filter on an Olympus fluorescent microscope. Three slides were used per sample, and three fields of view containing 200 cells were counted per slide.

The assay was performed after the haemocytes had been incubated in either PBS or antimycin for 2 hours.

2.3.7 Bacterial killing assay to measure the effect of antimycin on the destruction of pathogenic bacteria

To determine whether inhibition of the electron transport chain has a direct effect on the killing mechanism of haemocytes, a bacterial killing assay was performed using a modification of the method described by Volety *et al.* (1999). For the purposes of the assay, bacterial killing was defined as the inability of bacteria to proliferate in the presence of growth media after being exposed to haemocytes. The ability of the surviving bacteria to reduce MTT to a purple formazan was used as a measurement of the effect of the haemocytes on the bacteria. Thus, if the bacteria survived and proliferated, they would be able to reduce MTT to a purple formazan. The more bacteria that survived, the more formazan would be formed. There should be an inverse correlation between the ability of the haemocytes to kill the bacteria and the amount of formazan formed.

E. coli JM109 was cultured in 5 ml LB media at 37 °C overnight with shaking. The overnight culture was centrifuged at 3000 *x* g and resuspended in PBS to yield an OD of 0.5 (approximately 1 x 10^6 cells/ml). Haemocyte monolayers were incubated with 100 µl of the culture for 30 minutes to allow phagocytosis to occur. The bacterial cell suspension was then removed and the monolayers rinsed in PBS to remove any residual bacteria. Control samples, where haemocytes were merely rinsed with either 100 µl PBS or 100 µl antimycin, were used to represent incubation at T=0 hour. For the T=2 hour samples, haemocytes were incubated for two hours in either PBS (control samples) or 100 µl 100 µM antimycin (test samples). After incubation, the supernatant was removed and the haemocytes lysed by addition of 100 µl distilled water for 15 minutes. The lysed samples were transferred to 1.5 ml eppendorf tubes, 100 µl of LB media was added and the samples were incubated for 2 hours at 37 °C with shaking. Following incubation, 100 µl of MTT (5mg/ml) was added to each sample. After incubating for 2 hours in the dark, the bacterial cells were pelleted, the supernatant removed and the precipitated formazan dissolved by addition of 100 µl acidic isopropanol. Quantification of the formazan was performed spectrophotometrically at 540 nm using a Nanodrop® ND-1000 UV-Vis Spectrophotometer. The absorbance was used as a measure of bacterial viability, and thus survival of culturable bacteria and their ability to proliferate, after exposure to the

haemocytes. Higher absorbance values indicate that more bacteria are present after incubation in the growth media, and therefore the haemocytes in these samples had a decreased ability to kill bacteria.

2.4 Statistical Analysis

Data is shown as the mean of three biological repeats, each done in triplicate. Error bars represent the standard error of the mean. Where two means were compared, such as in the NBT assay, an unpaired student t-test was performed. For multiple comparisons, one-way ANOVA analysis was done using the Tukey method to test for significant difference, and $p<0.05$ was accepted as a signficant difference between values.

CHAPTER 3

RESULTS

CONTENTS

3.1 Confirmation of microarray

3.1.1 Semi-Quantitative PCR

The expression of cytochrome *b* and cytochrome *c* oxidase III in immune-stimulated abalone was studied using semi-quantitative PCR. The expression of both genes after probiotic feeding was compared to expression before immune-stimulation (T=0). The expression of actin, included as a housekeeping gene, was determined in all samples.

Expression of actin was not affected by probiotic feeding (3.1a) When the expression at T=0 (pre-feeding) is compared to the other time points (post-feeding), it can be seen that the average expression remains near 1 fold. The representative scan of the agarose gel shown in Figure 3.1b further highlights the constant expression of actin across all time points.

Although significant changes in expression of both cytochrome *b* and cytochrome *c* oxidase III was only observed after 48 hours (Figures 3.2 and 3.3 respectively) a similar pattern in expression change can still be observed. Expression of both genes increased steadily from 6 hours after feeding, peaked between 12 and 18 hours and decreased again at 36 hours post-feeding, finally showing a significant increase in expression 48 hours after probiotic feeding.

A)

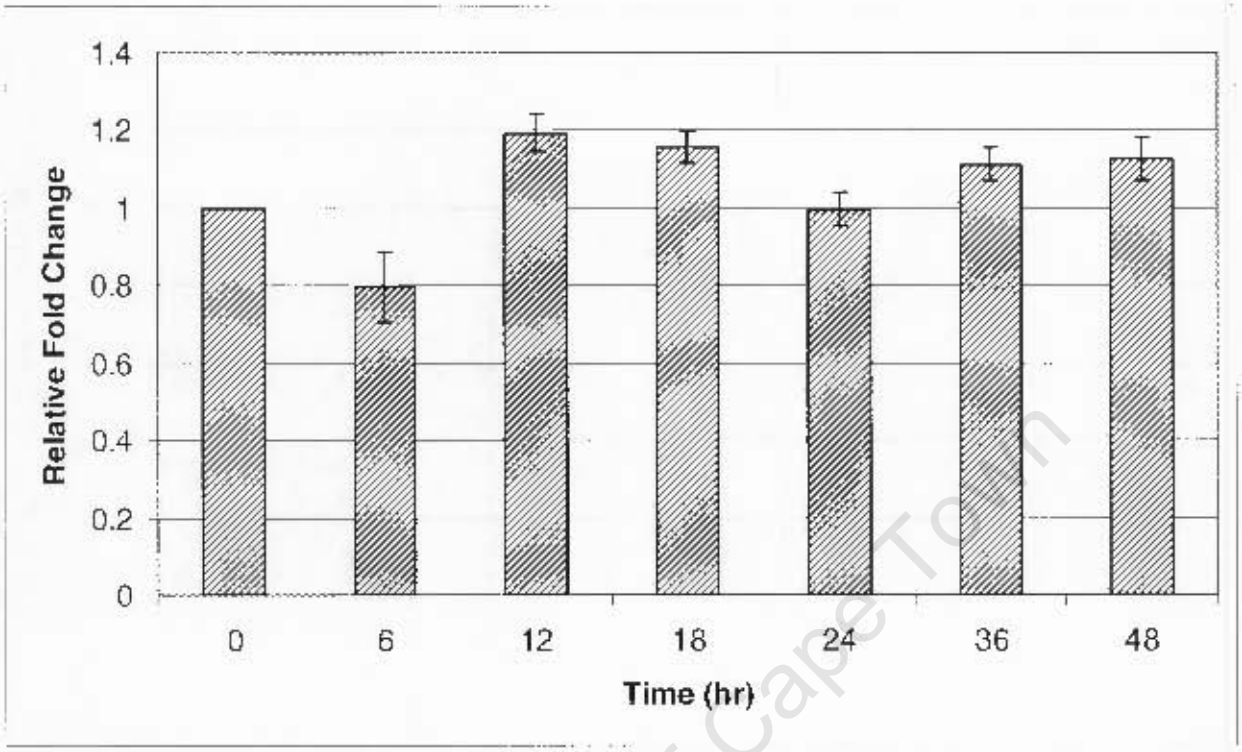

B)

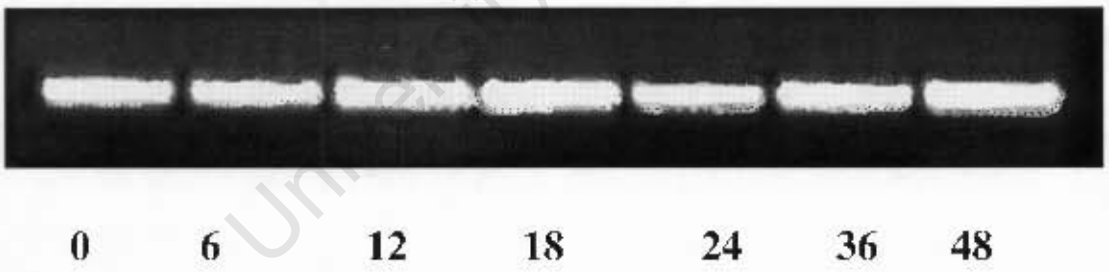

Figure 3.1 Semi-quantitative PCR of the housekeeping gene, actin. A) Relative fold change in expression of actin between T=0 and T=48. Each bar represents the mean of three technical repeats and the vertical lines represent standard error of the mean. B) Representative agarose gel showing expression of actin.

A)

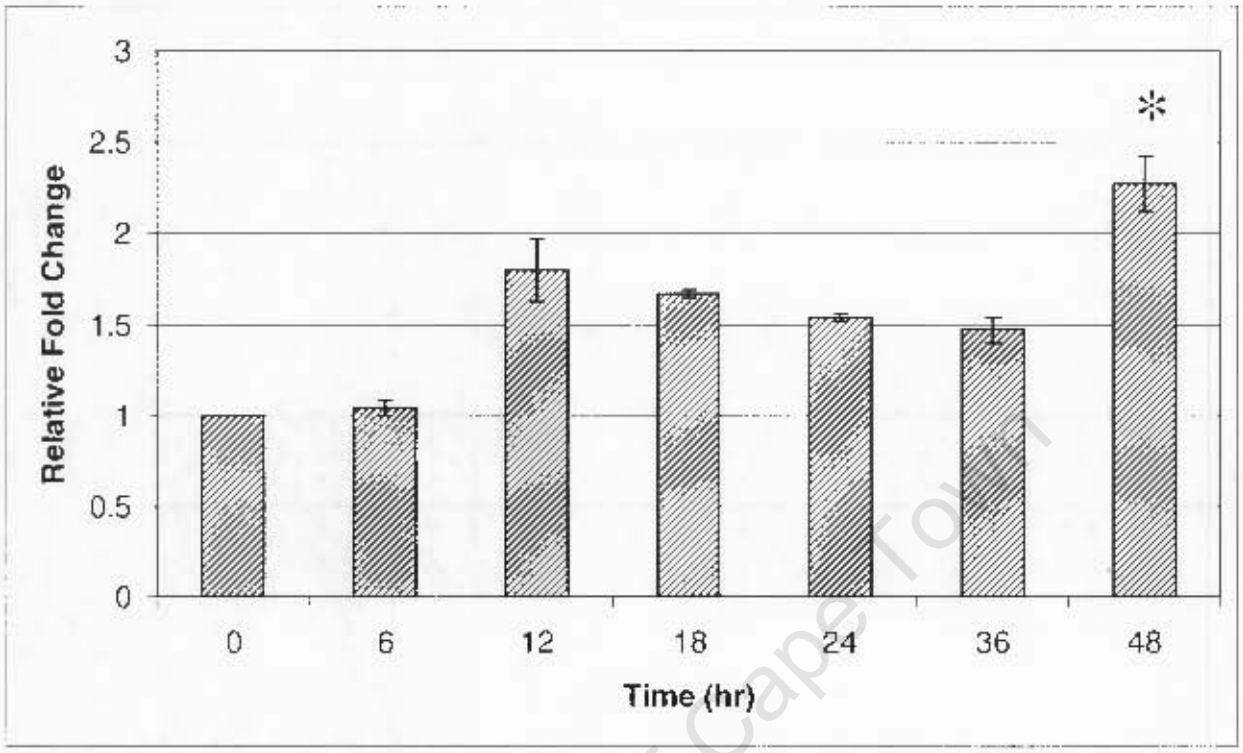

B)

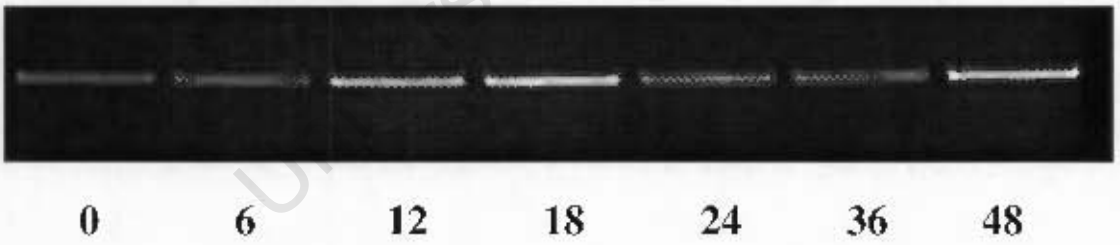

Figure 3.2 Semi-quantitative PCR of the cytochrome *b*. A) Relative fold change in expression of cytochrome *b* between 0 and 48 hours. Each bar represents the mean of three technical repeats and the vertical lines represent standard error of the mean. B) Representative agarose gel showing expression of cytochrome *b*. (*) indicates significant difference ($p < 0.05$) in gene expression in comparison to T=0.

A)

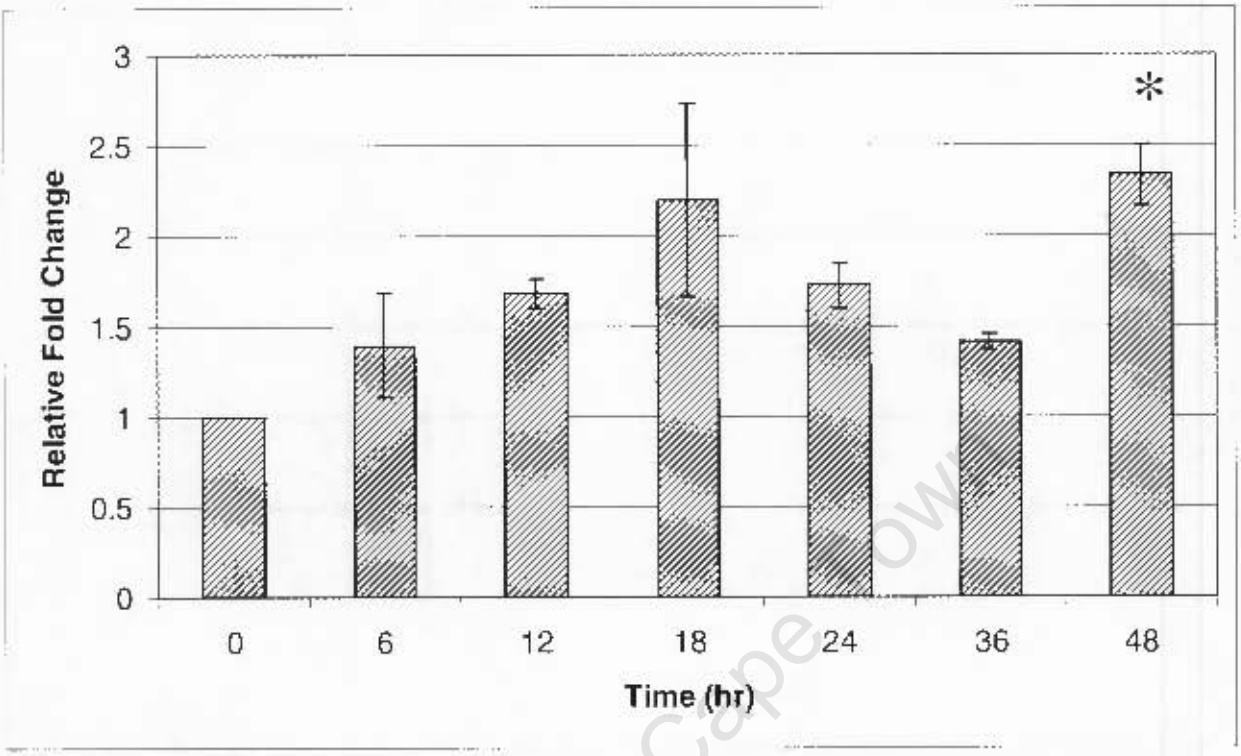

B)

0 6 12 18 24 36 48

Figure 3.3 Semi-quantitative PCR of the cytochrome *c* oxidase III. A) Relative fold change in expression of cytochrome *c* oxidase III between 0 and 48 hours. Each bar represents the mean of three technical repeats and the vertical lines represent standard error of the mean. B) Representative agarose gel showing expression of cytochrome *c* oxidase III. (*) indicates significant difference ($p < 0.05$) in gene expression in comparison to T=0.

Although the expression of cytochrome *b* is only significantly higher after 12 hours, a similar trend in expression is apparent with regard to both genes in that expression levels doubled in

comparison to T=0, after which time expression decreased slightly and doubled once again at T=48.

3.2 Determination of full length gene sequences and sequence analysis

3.2.1 Cytochrome *b*

The nucleotide sequence of a cDNA clone identified by microarray analysis as upregulated in immune-stimulated abalone (Arendze-Bailey, unpublished) was edited in DNAMan which resulted in a 730 bp sequence, which excludes the poly-A tail (Figure 3.4). A BLASTX search of the NCBI protein database revealed that this *Haliotis midae* sequence showed high similarity to the cytochrome *b* sequence of a number of gastropods, including black lip abalone (*Haliotis rubra)* to which it was 97% similar. The sequence also showed 74% similarity to that of the cone snail (*Conus textile*) and 70% similarity to that of a ribbon worm (*Cephalothrix rufifrons).* The sequence was approximately 60% similar to the cytochrome *b* sequence of various species of *Phlebotomus* sandflies. The results of the BLASTX search is shown in Table 3.1


```
1      GGGGGGGCTA CGGTAATTAC TAATCTTTTT TCTGCGGTTC CGTATATTGG GGGCGAGCTT
61     GTGCAGTGGA TGGGGGCGG ATTTGCGGTT GATAATGCTA CTTTAGTGCG GTTTTTTAGC
121    CTACATTTTT TGGTGCCATT TGTTATTGCT GGAATGAGGG TTCTTCATTT ATTATTCCTT
181    CACGAGACCG GGTCTAATAA TCCTTTGGGG CTAAACAGTG ATGGAGATAA GGTCCCATTT
241    CATTTTTATC ATACGGTTAA GGATTTAGTT GGATTCTTGG TTTTGTTATT TTTCTTAATG
301    TTGTTAGTGT TTTTTGACCC GTTTCTTTTA GGGGACCCGG AAAATTTTAT TCCGGCTAAT
361    CCGCTTGTTA CTCCAGTCCA TATTCAGCCT GAGTGGTATT TCTTATTCGC TTATGCTATT
421    TTACGGTCAA TCCCAAATAA GTTGGGCGGA GTAGTTGCCC TGGCGATGTC GGTGGTGATC
481    TTGTTTGTTG TTCCGCTGTT TCATTCCGGT AAATCACGAT CGTTCTGTTT TTATCCGTTG
541    AATCAAATTT TATTTTGGTG TTTTGTAGGT ATTCTGTTTA TTTTAACGTG GATTGGGGCA
601    TGTCCAGTTG AGCCGCCGTA TGAAGGAATT GGGCGAGTGT TTACTGTTCT CTATTTCGTG
661    TATTATTTAA TTAGCCCAAT ACTTCAGATA GTGTGGGATA GTATTCTTGA GTATTAGTTT
721    TTAAACCTGG AAAAAAAAAA AAAAAAAAAA AAAAAAAAAA
```

Figure 3.4 The nucleotide sequence (730 bp) of the cytochrome *b* gene of *Haliotis midae* obtained from the cDNA clone identified by microarray analysis (Arendze-Bailey, unpublished). The start (ATG) and stop (TAG) codons are indicated in bold.

Table 3.1 The top 10 protein sequence similarities obtained through a BLASTX search of the NCBI database using the 730 bp cytochrome *b* sequence from *Haliotis midae*

Species	**% Sequence similarity to *H. midae* cytochrome *b***	**Accession Number**
Haliotis rubra	97	YP_026076.1
Ilyanassa obsoleta	76	YP_492548.1
Lophiotoma cerithiformis	74	YP_635816.1
Cephalothrix rufifrons	71	ABM53206.1
Conus textile	70	YP_001004254.1
Cydistomyia duplonotata	68	YP_973152.
Eucalanus bungii	66	BAD18996.1
Phlebotomus perniciosus	65	AAD44996.1
Phlebotomus langeroni	64	AAD44999.
Phlebotomus orientalis	64	AAD44993.1

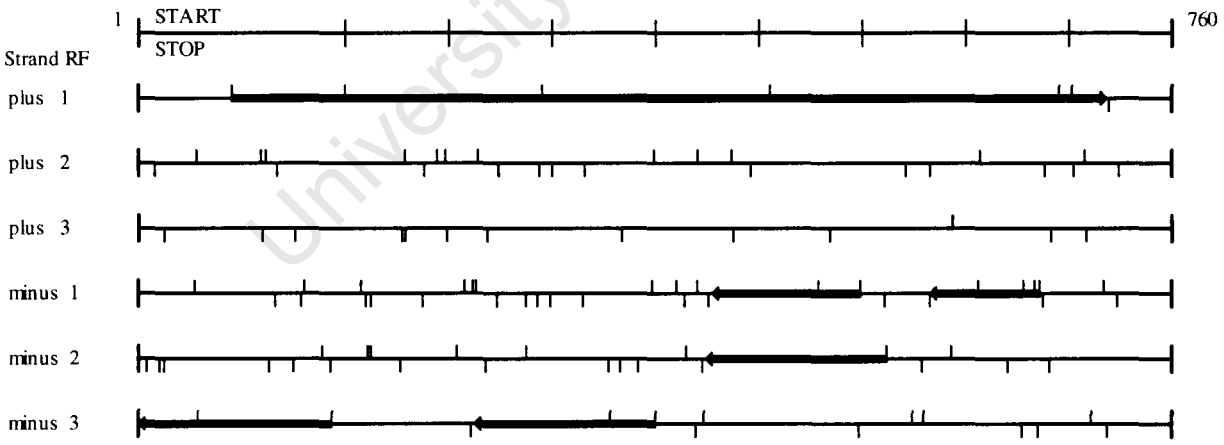

Figure 3.5 Open reading frames identified in the nucleotide sequence of the cytochrome *b* gene using an invertebrate mitochondrial translation table. The shaded area in reading frame +1 indicates the open reading frame that was used to derive the putative amino acid sequence of *H. midae* cytochrome *b*.

Using the open reading frame search function on the NCBI website, a single open reading frame was identified in the first reading frame of the nucleotide sequence, shown in Figure 3.5. This sequence was used to derive a putative 215 amino acid sequence for *Haliotis midae* cytochrome *b*, shown in Figure 3.6. Other open reading frames were also identified in the negative strand, but these were short and when subjected to a BLASTX search, did not show sufficient similarity to a known protein.

MWGGFAVDNATLVRFFSLHFLVPFVIAGMSVLHLLFLHETGSN*NPLGLNSDGDKVPFHFYHTVKDLVGFLVLLFFLM LLVFFDPFLLGDPENFIPANPLVTPVHIQPEWYFLFAYAILRSIPNKLGGVVALAMSVVILFVVPLFHSGKSRSFCF YPLNQILFWCFVGILFILTWIGACPVEPPYEGIGRVF*TVLYFVYYLISPMLQMVWDSILEY

Figure 3.6 Putative amino acid sequence of *Haliotis midae* cytochrome *b*. The N-terminal domain is indicated in bold, while the C-terminal domain is in underlined italics.

A search of the conserved protein domain database on the NCBI internet site (NCBI CDS BLAST) revealed that the putative cytochrome *b* amino acid sequence of *Haliotis midae* contained a partial cytochrome *b* N-terminus domain, as well as a complete cytochrome *b* C-terminus domain (Figure 3.7).

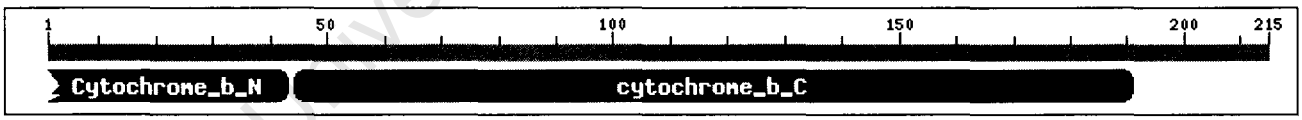

Figure 3.7 The partial N-terminus protein domain (cd00284.2) and complete C-terminus protein domain (cd00290.2) identified in the putative *Haliotis midae* cytochrome *b* amino acid sequence using CDS BLAST.

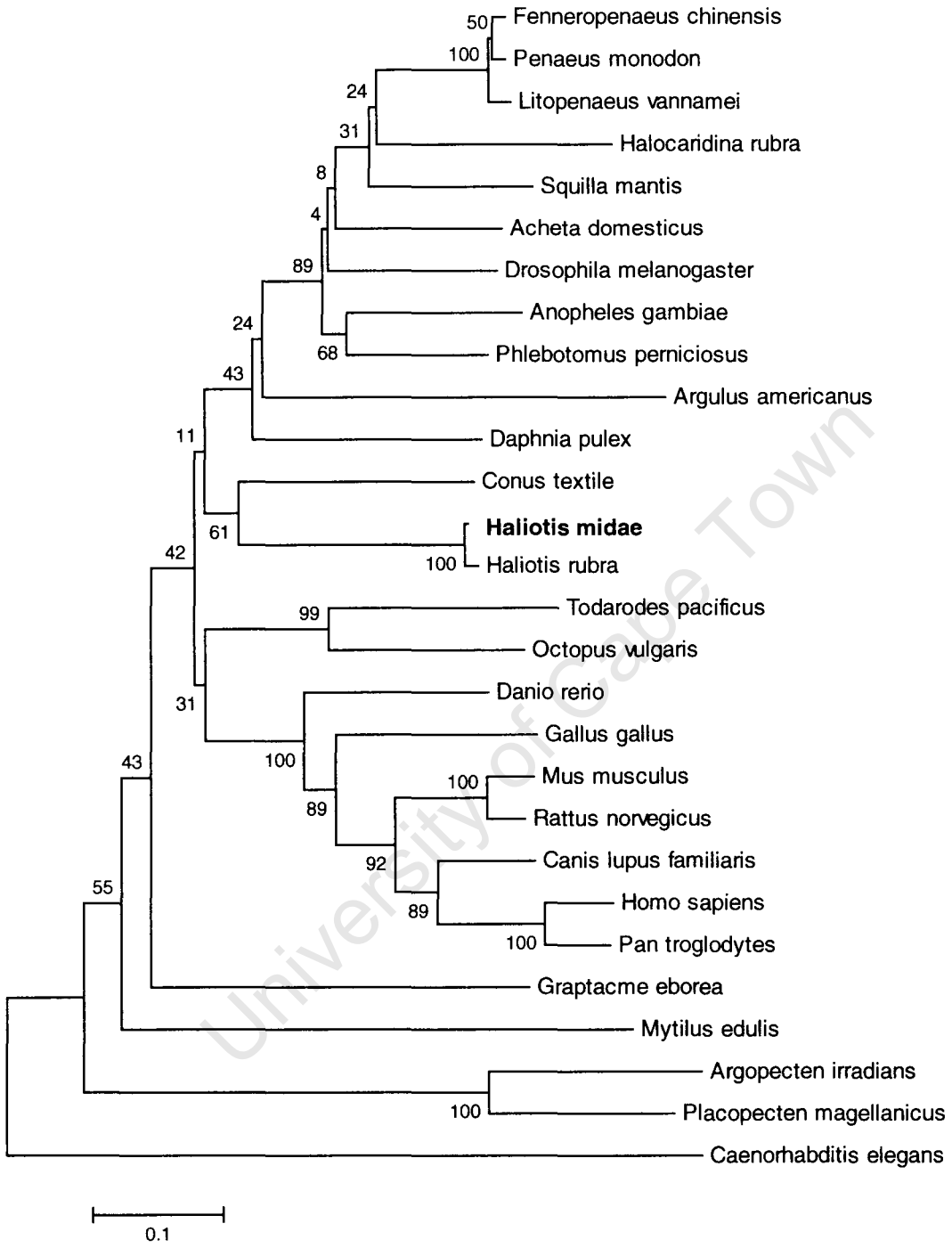

Figure 3.8 A phylogenetic tree derived from analysis of the putative cytochrome *b* amino acid sequence of *Haliotis midae*, and known cytochrome b sequences from 26 species using MEGA version 3.1. Numbers at the nodes indicate the bootstrap values retrieved from 500 replicates.

Phylogenetic analysis of the putative cytochrome b amino acid sequence from *Haliotis midae* (Figure 3.8) revealed that this sequence is very closely related to the cytochrome b sequence from the black lip abalone, *Haliotis rubra,* indicated by the bootstrap value of 100%, which confirms the results obtained from the BLASTX search shown in Table 3.1. The sequence was also related to cytochrome *b* of *Conus textile.* The sequence clustered near to the cytochrome *b* sequences of the cephalopods, whereas cytochrome *b* from other bivalve mollusks, such as *Mytilus edulis* seems to be less closely related, and clustered further away from the *Haliotis midae* branch.

3.2.2 Cytochrome *c* oxidase III

The nucleotide sequence of a cDNA clone identified by microarray analysis (Arendze-Bailey, unpublished) as upregulated in immune-stimulated abalone was edited in DNAMan which resulted in a sequence just more than 200 bp, including the poly-A tail (underlined in Figure 3.9). When this sequence was used in a BLASTX search of the NCBI protein database, it was revealed to be the 3' end of cytochrome *c* oxidase III. 5' RACE was used to find the remainder of the nucleotide sequence (rest of sequence in Figure 3.9). The two sequences were assembled in DNAMan, and a BLASTX search of the NCBI protein database showed that this 810 bp sequence was 98% similar to the full length cytochrome *c* oxidase III sequence of *Haliotis rubra* (Table 3.2). The *Haliotis midae* sequence also showed similarity to the cytochrome *c* oxidase III protein sequences of a number of gastropods, including *Lophiotoma,. cerithiformis, Ilyanassa.obsolete* and *Conus textile.* The assembled sequence also showed some similarity to cytochrome *c* III oxidase from the cephalopod *Nautilus macromphalus* and the spoonworm *Urechis caupo.*

```
1       ATGACCCGAA GACCTTTTCA TCTTGTCGAG TTTAGACCAT GGCCATTAAC TGGATCCGTG
61      GGAGCACTTT TTTTAACAGC CGGAACAGCC GGGTGGATAC ACGGACACCC TACAATAATT
121     CCAATCTTAG GAACGGTACT AATCATCTTA ACAATAATTC AATGATGACG TGATGTGGTC
181     CGAGAAGGAA CATTCCAAGG ATTTCACACA ACCAACGTAG CCTCAGGCCT ACGATGGGGT
241     ATAATCTTAT TCATTGTATC AGAAGTATGC TTCTTCTTTG CCTTTTTTTG AGCCTATTTC
301     CACAGAAGAT TGGCCCCAAC CCCAGAACTT GGCTCTGCCT GGCCCCCAAC CGGAATCTCC
361     CCTCTCAATC CCTTTCAAGT TCCCCTTCTC AACACTGCCG TACTTCTAGC ATCTGGAGTC
421     ACAGTAACCT GAGCCCACCA CAGAATCTTA GAAGGAGATA AAAAAGAAAG GTTCCAAAGA
481     CTTCTTTTGA CTGTCATCCT AGGAGCCTAC TTCACATTTC TCCAGGCAGG GGAATACATC
541     GAAGCCCCTT TTACAATCGC AGACGGAGTT TACGGATCTA CATTCTACGT AGCCACCGGA
601     TTCCACGGCC TACACGTACT TATTGGAACT ACATTCCTAA TTGTCTGCCT AGTTCGACTC
661     TATGCAAATC ACTTTTCAAC TGGGCATCAC TTCGGCTTCG AAGCAGCTGC ATGATATTGA
721     CATTTTGTAG ACGTAGTATG GCTATTCCTG TACCTCTCAA TTTATTGATG AGGATCTTAA
781     AACAACAATA AACCGTTCTA CTTTACAAAA AAAAAAAAAA AAAAAAAAAA AAAAA
```

Figure 3.9 The nucleotide sequence (810 bp) of the cytochrome *c* oxidase III gene of *Haliotis midae*. The underlined area indicates the sequence obtained from the cDNA clone, while the rest of the sequence was obtained through 5' RACE. The start (ATG) and stop (TAA) codons are indicated in bold.

Table 3.2 The top 10 protein sequence similarities obtained through a BLASTX search of the NCBI database using the 730 bp cytochrome *c* oxidase III sequence from *Haliotis midae*

Species	**% Sequence similarity to *H. midae* cytochrome *c* oxidase III**	**Accession Number**
Haliotis rubra	98	YP_026066.1
Lophiotoma cerithiformis	80	YP_635820.1
Ilyanassa obsolete	79	YP_492552.1
Clymenella torquata	78	YP_089675.1
Conus textile	78	YP_001004258.1
Cephalothrix rufifrons	77	ABM53211.1
Nautilus macromphalus	77	YP_133779.1
Urechis caupo	74	YP_588219.1
Alosa pseudoharengus	74	YP_001293651.1
Platynereis dumerilii	73	NP_009242.1

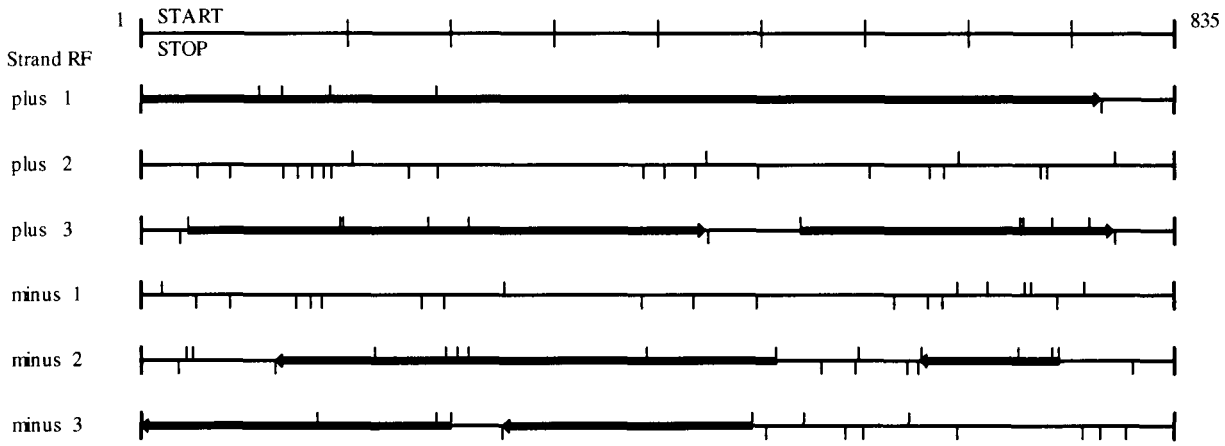

Figure 3.10 Open reading frames identified in the nucleotide sequence of the cytochrome *c* oxidase III gene using an invertebrate mitochondrial translation table. The shaded area in reading frame +1 indicates the open reading frame that was used to derive the putative amino acid sequence of cytochrome *c* oxidase III.


```
MTRSPFHLVEFSPWPLTGSVGALFLTAGTAGWMHGHPTMIPILGTVLIILTMIQWWRDVVREGTFQGFHTTNVASGL
RWGMILFIVSEVCFFAFFWAYFHSSLAPTPELGSAWPPTGISPLNPFQVPLLNTAVLLASGVTVTWAHHSILEGDKK
ESFQSLLLTVILGAYFTFLQAGEYIEPFTIADGVYGSTFYVATGFHGLHVLIGTTFLIVCLVRLYANHFSTGHHFGF
EAAAWYWHFVDVVWLFLYLSIYWWSGS
```

Figure 3.11 Putative amino acid sequence of *Haliotis midae* cytochrome *c* oxidase III.

Figure 3.12 The cytochrome *c* oxidase III protein domain (pfam cd01665) identified in the putative cytochrome *c* oxidase III amino acid sequence of *Haliotis midae* through NCBI CDS BLAST (http://www.ncbi.nlm.nih.gov/Structure/cdd/wrpsb.cgi)

Using the open reading frame search function on the NCBI website, a single open reading frame was identified in the first reading frame of the nucleotide sequence, shown in Figure 3.10. This open reading frame was used to derive a 258 amino acid sequence for the putative *H. midae* cytochrome *c* oxidase III, shown in Figure 3.11. Other open reading frames were also identified in the negative strand, but these were short and when subjected to a BLASTX search, did not show sufficient similarity to a known protein. A search of the conserved protein domain database on the NCBI internet site (NCBI CDS BLAST) revealed that the putative cytochrome *c* oxidase III amino acid sequence of *H. midae* contained a full cytochrome c oxidase III protein domain (Figure 3.12), further confirming that the full length sequence had indeed been obtained.

Phylogenetic analysis of the putative cytochrome c oxidase III amino acid sequence from *Haliotis midae* (Figure 3.13) revealed that this protein is very closely related to the cytochrome c oxidase III from the black lip abalone, *Haliotis rubra,* indicated by a bootstrap value of 100%. *H. midae* cytochrome *c* oxidase III is also closely related to other gastropods, such as *Conus textile,* which correlates to the results of the BLASTX search shown in Table 3.2. In fact, cytochrome c oxidase III from *H. midae* was nearly 80% related to the proteins from all vertebrates and invertebrates included in the analysis, with bootstrap values of 81 and 78% respectively.

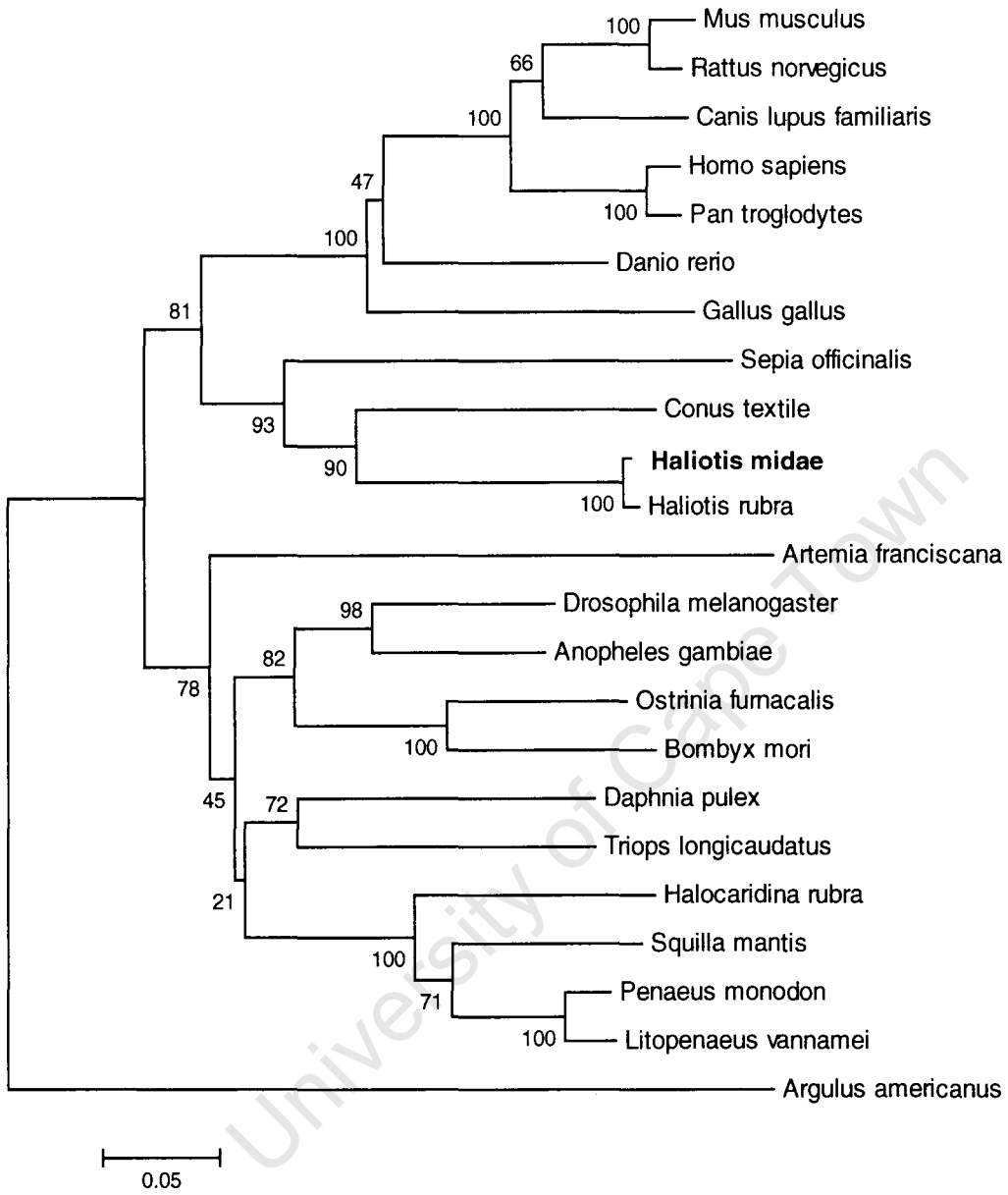

Figure 3.13 A phylogenetic tree derived from analysis of the putative cytochrome *c* oxidase III amino acid sequence of *Haliotis midae*, and known cytochrome b sequences from various species using MEGA version 3.1. Numbers at the nodes indicate the bootstrap values retrieved from 500 replicates.

3.3 The role of cytochrome *b* and cytochrome *c* oxidase III in the immune response of *Haliotis midae*

3.3.1 ATP assay to measure the effect of antimycin on electron transport

The effect of antimycin on the level of cellular ATP in haemocytes was measured using a luciferin/luciferase assay (Figure 3.14).

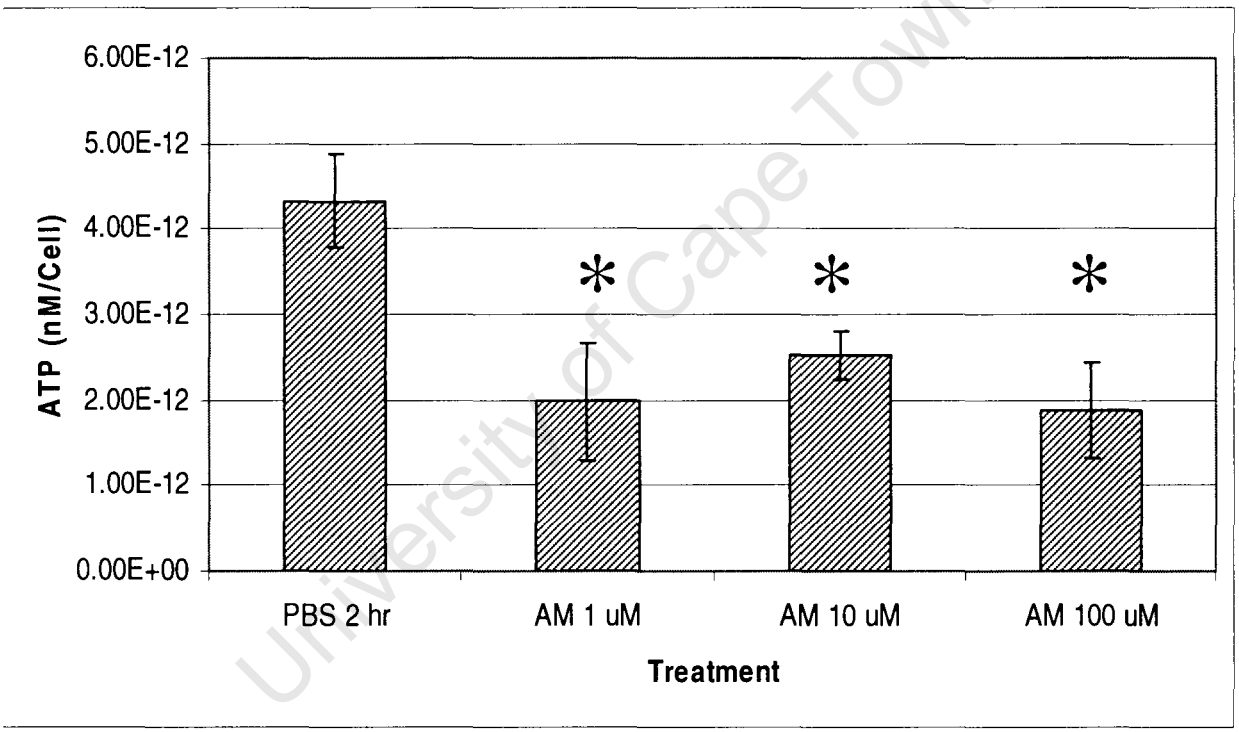

Figure 3.14 The effect of increasing concentrations of antimycin (AM) on the production of cellular ATP. Control samples were taken 2 hours after incubation in PBS (PBS 2 hr). Haemocytes were treated for 2 hours with 1 uM, 10 uM and 100 uM antimycin. The results are shown as nM ATP/cell and represent the mean of 3 biological repeats containing 3 technical repeats each ± standard error of mean. (*) indicates a significant difference ($p < 0.05$) compared to the PBS control.

The ATP present in the haemocytes treated with 1 uM antimycin, was approximately the same as the ATP concentration in haemocytes exposed to 10 uM and 100 uM antimycin, that is, 2 x 10^{12} nM ATP/cell. This concentration was nearly half that present in the control sample, which contained more than 4 x 10^{12} nM ATP/cell. This indicated that antimycin lea to a significant decrease in the levels of cellular ATP in treated haemocytes.

3.3.2 MTT (3-(4,5-Dimethylthiazol-2-yl)-2,5-diphenyltetrazolium-bromide) assay to measure the effect of antimycin on haemocyte viability

The effect of incubation with antimycin for 2 hours on the viability of haemocytes was determined by means of an MTT reduction assay (Figure 3.15). The viability was expressed as absorbance of the formazan that is formed when MTT is reduced. The ability of haemocytes incubated in PBS to reduce the MTT to a purple formazan was compared to that of haemocytes incubated in 1 uM, 10 uM and 100 uM antimycin.

Antimycin A had no significant effect on haemocyte viability in that the amount of formazan formed by antimycin A treated haemocytes was not significantly different to that of the control haemocytes (Figure 3.15) The effect of the ethanol in which the antimycin was dissolved was also determined. The viability of haemocytes incubated in 0.1 ul ethanol (equivalent to that in 10 uM antimycin) and 1 ul ethanol (equivalent to that in 100 uM) was not significantly reduced, and the amount of formazan formed was similar to the amount present in the control PBS sample.

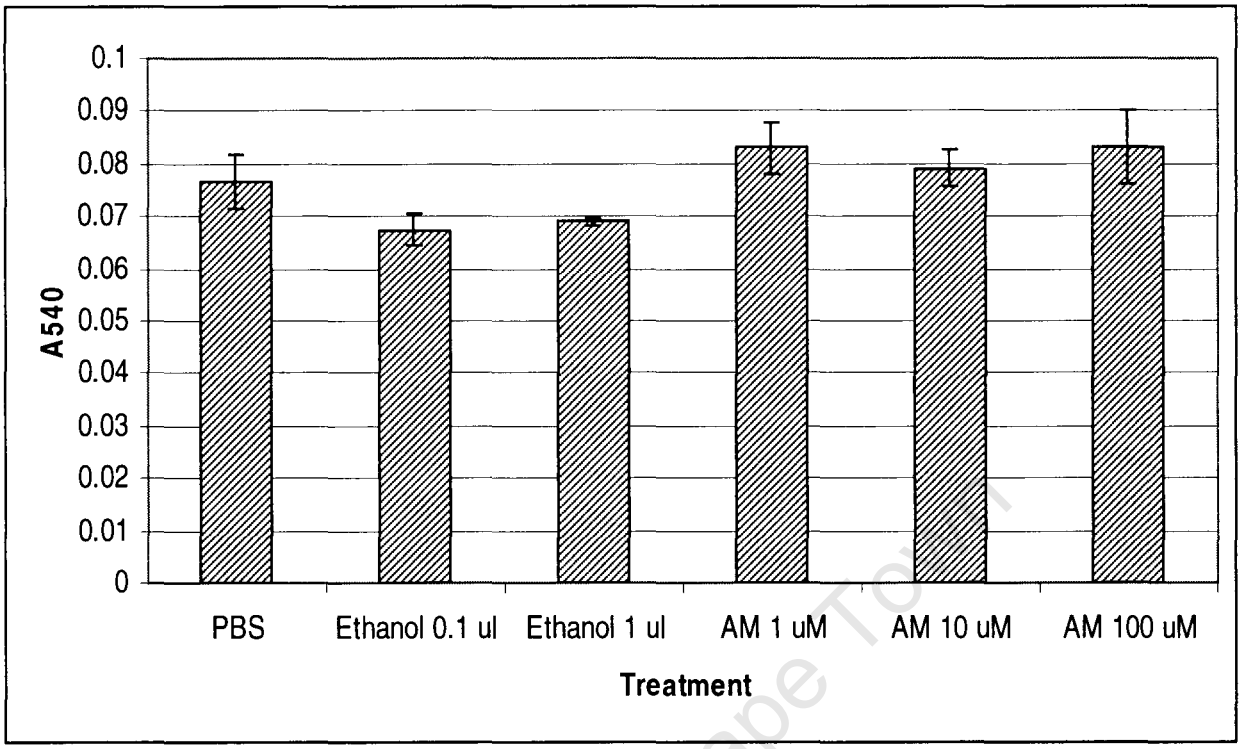

Figure 3.15 The effect of increasing concentrations incubation with antimycin (AM) for 2 hours on the ability of haemocytes to reduce MTT. Control samples were incubated with PBS, as well as 0.1 ul and 1 ul of ethanol in PBS. Test samples were incubated with 1 uM, 10 uM and 100 uM of antimycin. The results represent the mean absorbance of 3 biological repeats, each with 3 technical repeats ± standard error of mean.

3.3.3 NBT (Nitroblue Tetrazolium) assay to measure the effect of antimycin on the production of cellular superoxide anion in haemocytes

An NBT assay was used to determine what effect treatment with antimycin would have on the levels of cellular superoxide anion present in the haemocytes (Figure 3.16). The superoxide anion present in haemocytes incubated in PBS was compared to that present in haemocytes incubated in 100 uM antimycin. The addition of antimycin led to a significant increase in the level of superoxide anion, with the absorbance of the formazan increasing from 0.057 absorbance units to 0.088 absorbance units, which means that there was a 0.6 times increase in

the amount of superoxide present in the haemocytes treated with antimycin compared to the control haemocytes.

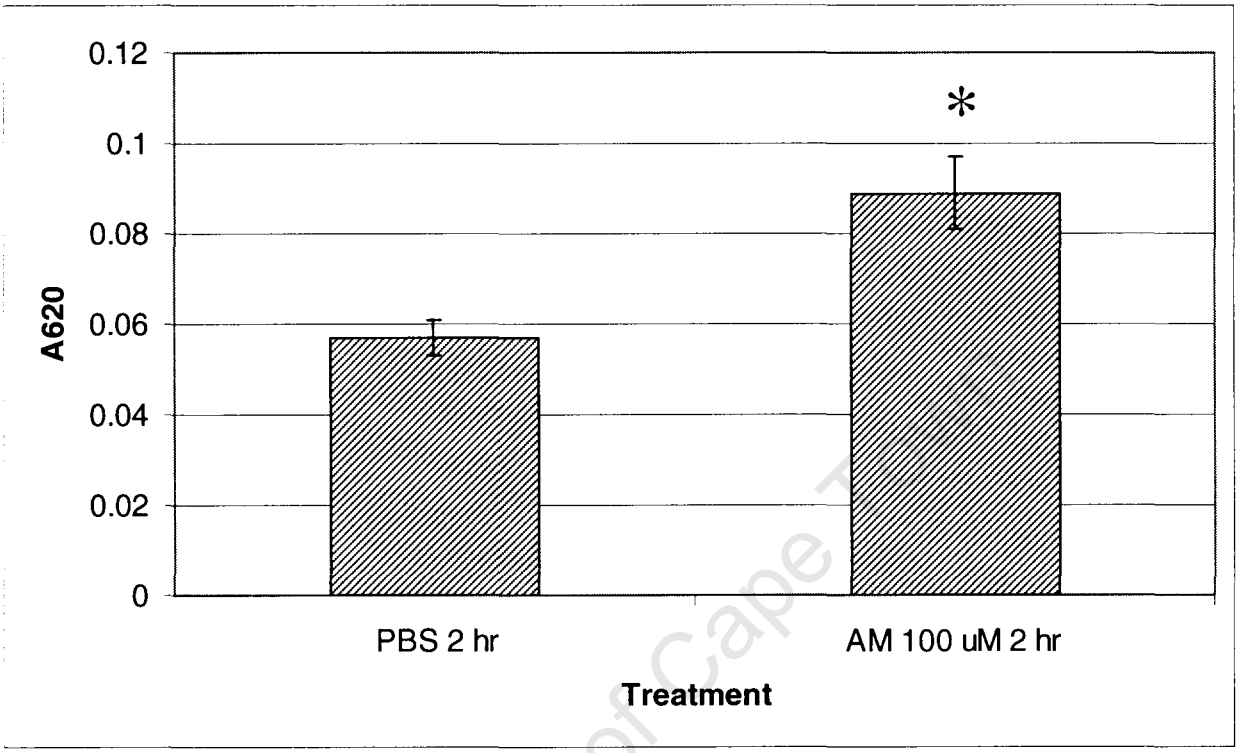

Figure 3.16 The effect of antimycin on the production of cellular superoxide after 2 hours of treatment as measured by the reduction of NBT. The control sample was incubated in PBS and the test sample in 100 uM antimycin (AM). The results represent 3 biological repeats with 3 technical repeats each and are shown as the mean absorbance ± standard error of mean. (*) indicates a significant difference ($p < 0.05$) compared to PBS 2 hr.

3.3.4 Phagocytosis assay to measure the effect of antimycin on the removal of pathogenic bacteria by haemocytes

A phagocytosis assay was used to determine the effect of antimycin on the ability of haemocytes to remove pathogenic bacteria through phagocytosis (Figure 3.17).

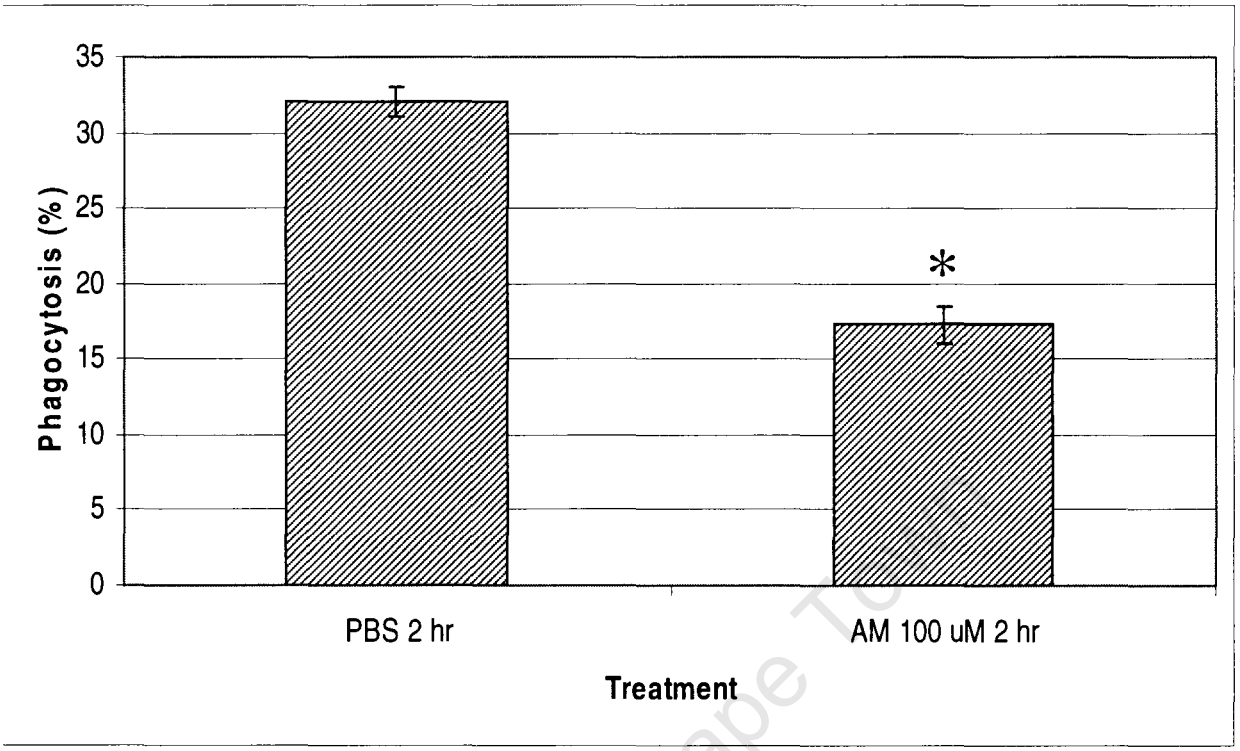

Figure 3.17 The effect of antimycin (AM) on the phagocytic activity of haemocytes 2 hours in PBS and test samples in antimycin. The results represent 3 biological repeats with 3 technical repeats each and are shown as the mean percentage phagocytosis ± standard error of mean. Different letters indicate a significant difference ($p < 0.05$) in values.

The percentage phagocytosis measured in haemocytes treated for 2 hours with antimycin was significantly lower than any of the other treatments, decreasing from between 30 % (PBS treated samples) and 25 % (samples treated with antimycin during attachment) to nearly 17% (Figure 3.17). Thus treatment with antimycin for 2 hours almost halved the phagocytic ability of the haemocytes.

3.3.5 Bacterial killing assay to measure the effect of antimycin on the destruction of pathogenic bacteria by haemocytes

To establish whether antimycin has an effect on the ability of haemocytes to destroy pathogenic bacteria, a MTT-based bacterial-killing assay was performed. This assay measures the amount of formazan formed by bacteria that survive exposure to haemocytes as an index of the amount of bacteria killed by the haemocytes. A high absorbance reading would thus indicate the presence of a larger number of viable bacteria than a sample with a lower absorbance reading.

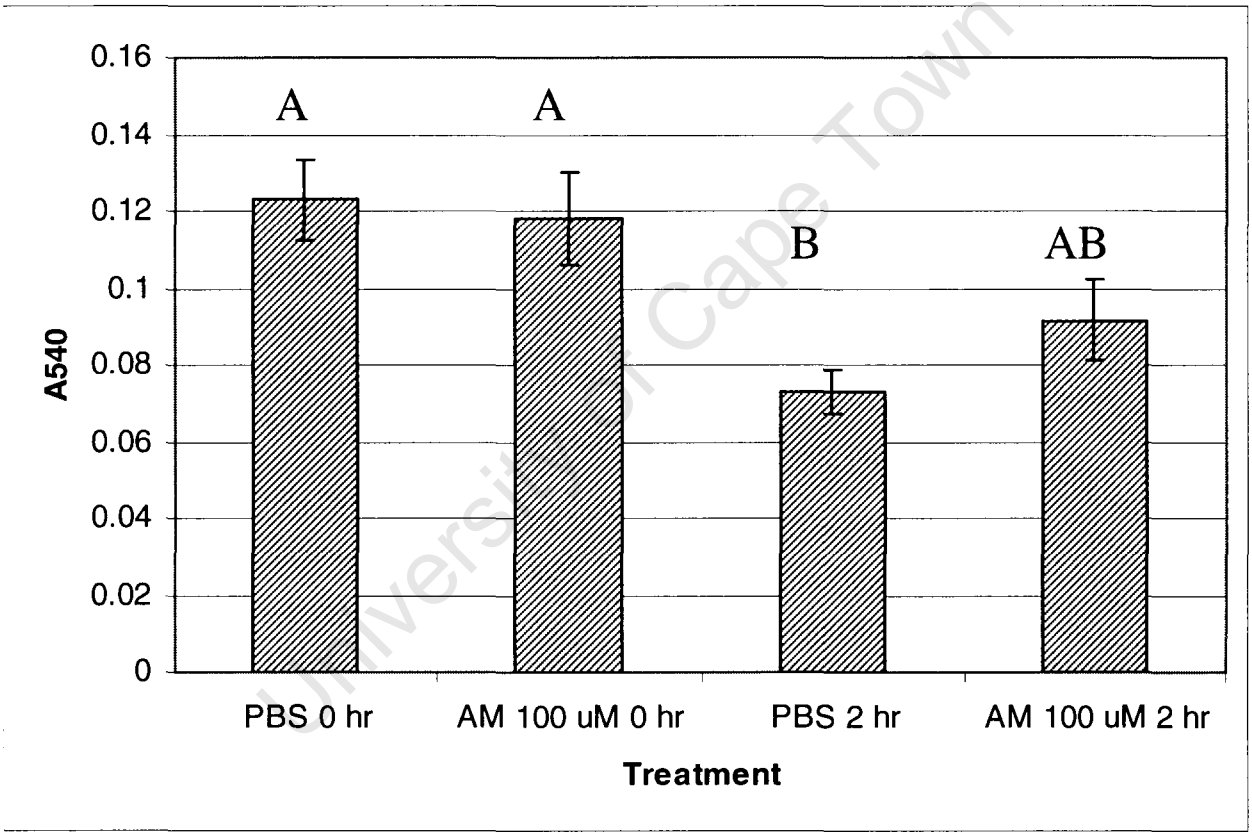

Figure 3.18 The effect of antimycin (AM) treatment on the ability of haemocytes to kill invading bacteria. Control samples were incubated in PBS for 0 and 2 hours (PBS 0 hr and PBS 2 hr respectively). Test samples were incubated in 100 uM antimycin for 0 and 2 hours. The results represent 3 biological repeats with 3 technical repeats each, and are shown as the mean absorbance ± standard error of mean. Different letters indicate a significant difference ($p < 0.05$) in values.

The number of bacteria killed by haemocytes incubated for 0 hours in PBS did not differ significantly from that observed in haemocytes incubated in antimycin for the same time, with the absorbance of the formed formazan being approximately 0.12 absorbance units (Figure 3.18). The number of bacteria remaining after 2 hours of exposure to haemocytes in PBS was significantly less than that in either of the 0 hour samples (PBS or antimycin), with the absorbance almost halving to approximately 0.07 absorbance units. The number of bacteria that survived exposure to haemocytes incubated in antimycin for 2 hours was not significantly less than that present in the samples incubated for 0 hours in antimycin or significantly more than to the number of viable bacteria associated with haemocytes incubated for 2 hours in PBS.

CHAPTER 4

DISCUSSION

CONTENTS

The South African abalone farming industry is the second largest outside Asia (Troell *et al.*, 2006). Wild-stocks have been depleted by over-fishing and uncontrolled poaching (Troell *et al.*, 2006) which has led to the rapid development of commercial abalone farming (Troell *et al.*, 2006). Farming of abalone generates direct permanent employment and thus contributes to the South African economy (Troell *et al.*, 2006), but the sustainability of this industry, and other commercial aquaculture industries, is threatened by the outbreak of numerous diseases (Miahle *et al.*, 1995). In order to combat disease, knowledge of how abalone respond to pathogenic invaders is required (Bachere, 2003). The aim of this study was to further our understanding of the abalone immune system by investigating the role of the electron transport system in the abalone immune response, and the reliance of this response on oxidative phosphorylation.

4.1 Analysis of cytochrome *b* and cytochrome *c* oxidase III gene expression in immune-stimulated abalone through semi-quantitative PCR

Semi-quantitative PCR is a method that is widely used to confirm results obtained from cDNA microarrays (Hsieh *et al.*, 2003, Tanguy *et al.*, 2004), EST libraries (Oh et al., 2006) or to study the expression profiles of individual genes (Fan *et al.*, 2007, Jiravanichpaisal *et al.*, 2007, Song *et al.*, 2006, Tian *et al.*, 2004, Wongprasert *et al.*, 2007). Semi-quantitative PCR requires the use of a housekeeping gene in order to avoid reporting false estimates regarding the abundance of the target genes (Chena *et al.*, 2005). For the study of expression of cytochrome *b* and cytochrome *c* oxidase III in *Haliotis midae,* actin was used as a housekeeping gene. As the expression of actin did not vary over the course of the experiment as shown in Figure 3.1, any changes in expression of cytochrome *b* and cytochrome *c* oxidase III could therefore be accepted as being due to immune-stimulation and not due to experimental error, inconsistent amplification during PCR or uneven loading of the agarose gels.

Although significant changes in expression only occurred 48 hours post-feeding, semi-quantitative PCR of RNA isolated from haemocytes from immune-stimulated abalone shows that both cytochrome *b* and cytochrome *c* oxidase III expression changed in response to feeding with probiotic-supplemented kelp cakes (Figure 3.2 and 3.3. respectively). Cytochrome *c* oxidase III responded more rapidly than cytochrome *b*, and was upregulated as early as 6 hours after

probiotic feeding was initiated. Upregulation of cytochrome *b* was initiated 12 hours after probiotic feeding began. Both genes remained upregulated 18 hours after feeding, and after a slight decrease in expression, a higher expression was observed 48 hours after probiotic feeding had begun. Although the expression of the genes did not exactly match, a similar pattern of expression could be observed. The expression of these two genes could be said to reflect the activity of the entire electron transport chain in the haemocytes in response to immune-stimulation through feeding with probiotic-supplemented kelp cakes because oxidative phosphorylation and the expression of the mitochondrial genome are interconnected (Garnik *et al.*, 2006) and also, it has been shown that the expression of the subunits of the respiratory complexes reflects the expression of the whole complex (Lienard *et al.*, 2006).

Upregulation of cytochrome *b* and cytochrome *c* oxidase III may occur when the metabolic requirements of the cell changes (Yin *et al.*, 1999) as a result of various stimuli. This has been shown in the termite *Reticulitermis santoriensis* (Lienard *et al.*, 2006) where analysis performed on head cDNA revealed that cytochrome *c* oxidase III was differentially expressed between castes due to differences in metabolic needs. It has also been shown that expression of cytochrome *c* oxidase III changes during development (Cannino *et al.*, 2004, Paraonu et al., 2005) during states of wake and sleep (Cirelli and Tononi, 1998) and in response to chemical stimulation (Yin *et al.*, 1999). Cytochrome *b* expression is also related to changes in metabolism, such as during visual deprivation (Kaminska *et al.*, 1997) and by nitric oxide treatment (Guo *et al.*, 2001). The activity of cytochrome *b* has also been shown to be affected by light irradiation (Tazawa *et al.*, 1996). Expression of cytochrome *b* and cytochrome *c* oxidase III in immune-stimulated abalone might therefore be related to changes in the metabolic needs of the abalone. As the immune response initiates, more metabolic energy is needed, and therefore the activity and expression of the components of the electron transport chain is increased.

4.2 Determination of full length gene sequences, sequence analysis and phylogenetic relationship of *Haliotis midae* cytochrome *b* and cytochrome *c* oxidase III

Analysis of the cytochrome *b* sequence, obtained from the cDNA clone, and the cytochrome *c* oxidase III sequence, obtained from the cDNA clone and 5' RACE, was performed to elucidate the putative amino acid sequences and protein domains, and to establish the phylogenetic relationship between cytochrome *b* and cytochrome *c* oxidase III from *Haliotis midae,* and those from organisms found to have the most sequence similarity.

The cytochrome *b* sequence obtained from the cDNA library clone was 730 bp long, and contained a single, 644 bp open reading frame, coding for 215 amino acids. The cytochrome *b* protein sequences listed in Table 3.1 are all approximately 370 amino acids long. Similarly, other cytochrome *b* sequences, such as those from crustaceans (Tjensvoll *et al.*, 2005), have also been shown to be this size. The shorter length of the *Haliotis midae* sequence was explained when a search for conserved protein domains using the NCBI internet site found two domains, a partial N-terminal protein domain, which contains heme-binding sites (Tjensvoll e*t al.*, 2005), and a complete C-terminal protein domain, which contains the ubiquinol/ubiquinone binding sites (Tjensvoll *et al.*, 2005). The partial N-terminal domain would explain the shorter length of the *Haliotis midae* sequence. It might thus be possible that the amino acid sequence obtained in the current study is that of the C-terminal domain and that the start codon for the N-terminal domain lies upstream of this sequence.

The cytochrome *c* oxidase III sequence, obtained from the *Haliotis midae* cDNA library and 5'RACE, was found to contain a complete cytochrome *c* oxidase III protein domain (Richter and Ludwig, 2003). The 730 bp open reading frame coded for a putative 258 amino acid sequence. This amino acid sequence is similar in length to the cytochrome *c* oxidase III sequence from other organisms, such as *Tigriopus japonicus* (265 amino acids (Tjensvoll *et al.*, 2005)) and *Penaeus monodon* (263 amino acids (Tjensvoll *et al.*, 2005)). In fact, the amino acid sequence of all the cytochrome *c* oxidase III proteins listed in Table 3.2 is approximately 260 amino acids in

length. The cytochrome *c* oxidase III nucleotide and amino acid sequences shown in Figures 3.9 and 3.11 respectively are therefore most probably the full sequences for *Haliotis midae.*

Phylogenetic analysis using the putative cytochrome *b* amino acid sequence from *Haliotis midae* showed that this protein has a high similarity to organisms belonging to related taxa, clustering on the same branch as *Haliotis rubra*, and very closely to other gastropods and to cephalopods (Figure 3.8). Similarly, cytochrome *c* oxidase III also shared a branch with *Haliotis rubra*, and clustered closely to other gastropods (Figure 3.13). The phylogenetic analysis of both cytochrome b and cytochrome c oxidase III gave similar results to that of the BLASTX search (Tables 3.1 and 3.2 respectively), with both genes showing the highest similarity to that of other abalone species and related gastropods.

4.3 The role of cytochrome *b* and cytochrome *c* oxidase III in the immune response of *Haliotis midae*

Semi-quantitative PCR showed that both cytochrome *b* and cytochrome *c* oxidase III are upregulated in response to immune stimulation. This implied that both genes, and therefore the mitochondrial respiratory chain, might play a role in the immune response of the abalone. Consequently, the role of the mitochondrial respiratory chain components, including cytochrome *b* and cytochrome *c* oxidase III, in the abalone immune response was investigated through inhibition of electron transport in abalone haemocytes. Electron transport was blocked by antimycin, a specific electron transport inhibitor, and the effect of this on immune parameters measured. Antimycin was chosen to study the effects of respiratory inhibition in haemocytes as it has been shown to decrease oxygen consumption (Sbarra and Karnovksy, 1959, Li *et al.*, 2007, Bermudez *et al.*, 1997) and lead to the rapid inhibition of oxidative metabolism (Gesinki, 1976) through inhibition of the activity of respiratory complex III (Li *et al.*, 2007).

Inhibition of electron transport through antimycin treatment has been shown to be harmful to cells by inducing apoptosis (Wolvetang *et al.*, 1994) and has been shown to lead to the death of numerous cell types including juxtaglomerular cells (Watabe and Nakaki, 2007), hepatocytes (Zhang *et al.*, 2001, Niknahad *et al.*, 1995) and human lymphoblastoid cells (Wolvetang *et al.*,

1994). It is thought that it is a combination of a decrease in ATP (Zhang *et al.*, 2001), increased superoxide production (Watabe and Nakaki, 2007) and the collapse of the proton motive force (Zhang *et al.*, 2001) that is responsible for cell death. It was therefore important to ensure that the haemocytes remain viable during the course of the assays employed in this study and that any reduction in immune response would be directly due to inhibition of electron transport, and not merely because the viability of the cells had been compromised and therefore all cellular activities, including those of the immune system, reduced.

The MTT assay was chosen to measure the effect of antimycin on haemocyte viability (Figure 3.15). The MTT assay is widely used to assay the viability of numerous cell types (Abe and Matuski, 2000, Young *et al.*, 2005, Lobner, 2000) including phagocytic cells (Molinari *et al.*, 2005) and to determine the effect of chemical treatment on cell viability (Chu *et al.*, 2002, Fotakis and Timbrell, 2006). After being incubated in antimycin for 2 hours, the treated haemocytes did not show a significant reduction in viability, demonstrated by their ability to reduce MTT to a formazan at the same level as the control haemocytes. The highest concentration of antimycin, 100 uM, together with an incubation time of 2 hours, did not negatively affect cell viability, and therefore these conditions were used in subsequent assays.

After establishing that antimycin did not have a negative effect on the viability of the haemocytes, the effect of the inhibitor on the final product of electron transport, namely ATP, was determined. Antimycin has been shown to lead to marked reductions in cellular ATP levels (Zhang *et al.*, 2001, Watabe and Nakaki, 2007, Niknahad *et al.*, 1995). Measuring the effect of antimycin on cellular ATP would assist in determining whether antimycin indeed has an inhibitory effect on the electron transport system of *Haliotis midae,* which was necessary as no information concerning the effect of antimycin on abalone haemocytes is available to date. It would also prove that decreases in immune related responses were due to inhibition of electron transport alone and not other unknown factors.

The level of ATP in haemocytes treated with antimycin was markedly decreased compared to that of control cells (Figure 3.14). In fact, the level of ATP in treated cells was almost 50% of that in control cells. This compares favourably with results from other cell types, such as

hepatocytes, where antimycin has been shown to lead to a 15% decrease in cellular ATP compared to control cells (Zhang *et al.*, 2001) and in renal epithelial cells, where ATP decreased by 40% compared to cells not treated with antimycin (Li *et al.*, 1993).

Concomitant to a decrease in the levels of cellular ATP, antimycin is known to lead to a significant rise in cellular superoxide anion production (Watabe and Nakaki, 2007). In abalone haemocytes, treatment with antimycin led to a significant rise in cellular superoxide anion, as measured using a NBT assay (Figure 3.16). The NBT assay has been shown to be useful in measuring the production of superoxide by various types of phagocytic cells, such as mouse macrophages (Choi *et al.*, 2006), shrimp (Munoz *et al.*, 2000), prawn (Soria *et al.*, 2006) and bivalve mollusc (Wootton and Pipe, 2003) such as oyster (Lacoste *et al.*, 2002), and specifically in abalone (Malham *et al.*, 2003)

The level of superoxide in haemocytes treated with antimycin rose by 60% compared to control cells. Superoxide anion was also detected in the control cells, but this effect has also been shown to occur in white shrimp, *Penaeus vannamei*, where haemocytes exhibited background superoxide production without receiving stimuli (Munoz *et al.*, 2000).

Production of high levels of superoxide due to antimycin treatment has been widely demonstrated (Niknahad *et al.*, 1995, Sierra *et al.*, 2005, Meany *et al.*, 2006) in various cell types (Niknahad *et al.*, 1995b, Watabe and Nakaki, 2007, Park *et al.*, 2007, Belyaeva *et al.*, 2006) and organisms (Garnik *et al.*, 2006,). Meany *et al.* (2006) showed that mitochondria treated with antimycin released five times more superoxide into the mitochondrial matrix compared to control samples. Mukhopadhyay *et al.* (2007) showed that a 3-7 fold dose-dependent increase in superoxide production occurred in response to antimycin in rat and human cells. This effect is explained by the fact that when electron transport along the respiratory chain is interrupted, formation of reactive oxygen species, such as superoxide anion, increases as a result of autoxidation of the reduced electron transport components (Siraki et al., 2002). The increased amount of superoxide has also been shown to be partially responsible for subsequent cell death due to oxidant stress (Zhang *et al.*, 2001, Watabe and Nakaki, 2007), and therefore the importance of ensuring that the haemocytes remained viable during treatment with antimycin

was once again highlighted. This extra pool of superoxide would later be observed to influence the results of the bactericidal assay, as superoxide has long been established as an anti-bacterial agent (Meany *et al.*, 2006) and is released by numerous marine invertebrates in response to bacterial infection (Chu *et al.*, 2002, Zelck *et al.*, 2005, Ksenzenko *et al.*, 1983, Bugge *et al.*, 2007, Munoz *et al.*, 2000).

As a direct measure of the importance of the electron transport chain in the immune response of the abalone, the effect of antimycin on phagocytosis was determined. Phagocytosis in haemocytes treated with antimycin declined from nearly 30% in control cells to 17% in treated cells (Figure 3.17). A similar effect has been shown in human monocytes, where treatment with antimycin led to a 50% decrease in phagocytosis after 45 minutes of incubation in 360 uM antimycin (Reiss and Roos, 1987) as well as in alveolar macrophages, where antimycin caused diminished phagocytosis of fluorescent beads (Kobzik *et al.*, 1990).

It has been shown that different types of phagocytic cells respond differently to antimycin, as demonstrated by Sbarra and Karnovksy (1959) as well as by Reiss and Roos (1987). In both these studies, antimycin depressed oxygen consumption in monocytes and nearly abolished phagocytosis, but had little or no effect on the leukocytes. Blecher and Goldstein (1977) also found that antimycin had a significant effect on phagocytosis in monocytes. It seems therefore that abalone haemocytes exhibit similar responses to monocytes, and that phagocytosis in abalone haemocytes might be dependent on a functional electron transport chain and oxidative phosphorylation.

After determining that a functional electron transport system is necessary for phagocytosis of invading pathogens, the effect of an inhibited electron transport system on the bactericidal action of abalone haemocytes was established. Killing of invading pathogenic microbes represents the ultimate defense capability of the host and integrates immune activities such as recognition, locomotion, membrane stimulation, attachment, phagocytosis and intracellular degradation (Volety *et al.*, 1999).

Bacterial killing by abalone haemocytes was estimated colorimetrically through the reduction of the tetrazolium salt MTT to a purple formazan (Volety *et al.,* 1999) (Figure 3.18). Volety *et al.* (1999) found that the absorbance of formazan produced during the assay is directly proportional to the number of bacterial colonies detected by agar plate count methods such as those described by Canesi *et al.* (2001, 2002). Thus, absorbance can be directly correlated to the number of bacterial colonies that survived exposure to the haemocytes.

The bactericidal assay showed that the number of bacteria that survived exposure to haemocytes that had been incubated in antimycin for 2 hours was not significantly less than in the controls. If antimycin had inhibited bacterial killing, one would expect that the number of surviving bacteria would be equivalent to that of the 0 hour control, as they represent starting bacterial numbers, and significantly higher than that in the 2 hour control which represents bacterial numbers following haemocyte killing. What the results do show is that some killing did occur, but not to the same level as that in the 2 hour control.

A possible explanation for this phenomenon could be, as mentioned earlier, the production of additional superoxide anion at complex III in response to antimycin blockage of electron transport. This superoxide is not produced as a physiological response to the invading bacteria, but due to leakage of electrons from complex III. Superoxide has been shown to be bactericidal (Gonzalez *et al.*, 2005) and is formed in response to bacterial invasion in numerous marine organisms such as *Crassostrea gigas* (Labreuche *et al.*, 2006), *Macrobrachium rosenbergii* (Sierra *et al.*, 2005), *Lynmaea stagnalis* (Zelck *et al.*, 2005) and *Mercenaria mercenaria* (Bugge *et al.*, 2007).

Non-oxygen dependent defense systems, which would have been active despite inhibition of the electron transport system, might also have played a role in the decreased number of bacteria in the sample treated with antimycin. These systems include cytotoxic factors such acid phosphatase (Cheng *et al.*, 2005, Hong *et al.*, 2006), lysozyme (Hong *et al.*, 2006, Cheng *et al.*, 1975) and peroxidase (Matricon and Letocart, 1999), which have all been identified in haemocytes of molluscs. They also include antimicrobial factors, such as antibacterial and

antifungal peptides, of which four types have been isolated from haemocytes in the bivalve Mytilus edulis (Charlet *et al.*, 1996, Mitta *et al.*, 2000).

Because of the interference of the superoxide with the bacterial killing assay, it is difficult to determine conclusively whether antimycin did or did not inhibit bacterial killing. Indeed, Watabe and Nakaki (2007) mention that superoxide production following treatment with respiratory inhibitors makes it difficult to analyse their effect on cellular functions. The results of the bactericidal assay do show that normal haemocytes do recognize and kill *E. coli* as an invading pathogen, and that antimycin leads to a large enough production of superoxide anion to destroy some of the invading bacteria. Since antimycin has been shown to interfere with the killing of *Staphylococcus* in alveolar (Kobzik *et al.*, 1990) and murine macrophages (Miller, 1971), and further investigation is required to unequivocally determine the effect of inhibition of the electron transport system on the bactericidal action of abalone haemocytes.

4.4 Conclusion and future work

This study has shown that expression of both cytochrome *b* and cytochrome *c* oxidase III is upregulated in immune-stimulated abalone, and that these genes, their protein products, and therefore the mitochondrial respiratory chain, plays a role in the immune response of the abalone due to the increased metabolic needs of the cell during immune-stimulation.

Future work might include *in situ* hybridization, which could be used to detect exactly where the cytochrome *b* and cytochrome *c* oxidase III genes are expressed during immune stimulation, and exactly when feeding with the probiotic-supplemented kelp cake induces the expression of these genes. This would be used to show in which cells metabolic activity is highest during immune stimulation *In situ* hybridization has been successfully performed in abalone where oligonucleotide probes were used to identify gut-flora (Tanaka *et al.*, 2004). *In situ* immunology could also be performed using antibodies, which would help to identify where the cytochrome *b* and cytochrome *c* oxidase proteins occur after immune-stimulation. The results from this experiment could be used to confirm the results of the semi-quantitative PCR performed in the current study.

RNA interference methods might be useful to explore the individual roles of cytochrome *b* and cytochrome *c* oxidase III in the immune response of the abalone, by investigating how the immune system would be affected if these genes were silenced individually or in concert. RNA interference has been successfully employed to silence immune-related genes in *Hyalophora cecropia* (Terenius *et al.*, 2007), and is used in marine shrimp to induce anti-viral immunity (Robalino *et al.*, 2007).

The effect of antimycin on the expression of cytochrome *b* and cytochrome *c* oxidase III *in vivo* could also be investigated, as it has been shown that inhibition of electron transport leads to an increase in both cytochrome *c* oxidase and cytochrome *b* (Garnik *et al.*, 2006). As treatment of abalone with antimycin might not be feasible in practice, exposing the abalone to hypoxia, which would also essentially inhibit electron transport, might prove successful, as studies in the grass shrimp, *Palaemonetes pugio* have shown that hypoxia leads to the expression of genes on the mitochondrial genome, including cytochrome *b* and cytochrome *c* oxidase (Garnik *et al.*, 2006).

A more comprehensive view of the effect of respiratory inhibition on the immune response might be obtained by measuring other immune parameters such as phenoloxidase, lectin binding, acid phosphatase and non-specific esterases (Wootton *et al.*, 2003). Alternative methods could be sought to assay the parameters measured in the current study. Phagocytosis and cell viability could be measured by flow cytometry, in a similar manner to Brousseau *et al.* (2000) and superoxide production could be measured by luminometry using chemiluminescence (Dahlgren and Karlsson, 1999). Alternative inhibitors of respiration, such as rotenone and cyanine (Ksenzenko *et al.*, 1983), which inhibit complex I and cytochrome *c* respectively, could be used to determine whether these inhibitors have the same effect as antimycin on the abalone immune response.

Knowledge of the abalone immune system is based on limited studies in abalone and variable amounts of work in other molluscs (Hooper *et al.*, 2007). Increasing our understanding of how the abalone immune system functions, specifically in response to probiotics, would prove helpful in better implementation of this alternative treatment to chemicals, which would not only be advantageous for the animals in question, but also for the environment in the long term.

APPENDIX A

MEDIA AND SOLUTIONS

CONTENTS

A.1 Media

A.1.1 Marine Broth with 1 % NaCl (MB)

NaCl (Saarchem)	30.0 g
$MgCl_2.6H_2O$ (Saarchem)	2.3 g
KCl (Saarchem)	0.3 g
Casamino Acids (Difco)	5.0 g
Yeast Extract (Biolab)	1.0 g
D-glucose (Saarchem)	2.0 g
dH_2O to	1 L

Autoclave

A.1.2 Yeast Tryptone Broth (YTB)

Tryptone	20 g
Glucose	20 g
Yeast	10 g
dH_2O to	1 L

Autoclave

A.1.3 Luria Broth (LB)

NaCl	10 g
Tryptone (Biolab)	10 g
Yeast Extract	5 g
dH_2O to	1 L

Autoclave

A.1.4 Kelp Cakes

Pre-Swollen Kelp (40%)	400 g
Agar (2%)	20 g
Sea Salts	1 L

Pre-Swollen kelp: Add 30 g/L NaCl to 100 g dry kelp. Allow to swell overnight at room temperature in a closed container. Autoclave after adding agar and sea salts.

A.1.5 Sea Salts

NaCl	30 g
$MgCl_2 . 6H_2O$	2.3 g
KCl	0.3 g
dH_2O to	1 L

Autoclave

A.2 Solutions for primary culture of haemocytes

A.2.1 Alsever's Buffer

Glucose	20.8 g
Na-Citrate	8 g
EDTA	3.36 g
NaCl	22.4 g
Formaldehyde (37 %)	120 ml
dH_2O to	1 L

Adjust pH to 7.5

A.2.2 Modified Hank's Buffer Salt Solution (MHBSS)

Glucose	10.4 g
NaCl	11.2 g
KCl	0.41 g
KH_2PO_4	0.1 g
$CaCl_2$	0.355 g
$MgCl_2$	1.31 g
$MgSO_4$	1.573 g
EGTA	0.015 g
dH_2O to	1 L

Adjust pH to 7.2
Autoclave

A.2.3 Phosphate Buffer Saline (PBS)

NaCl	8 g
KCl	0.2 g
Na_2HPO_4	1.44 g
dH_2O to	1 L

Adjust pH to 7.4 with HCl
Autoclave

A.3 Solutions for gel electrophoresis

A.3.1 Tris/Acetate/EDTA (TAE) 50 x stock

Tris-base (Roche)	242 g
Glacial acetic acid (Saarchem)	57.1 g
EDTA (0.5 M, pH 8) (Saarchem)	100 ml
dH_2O to	1 L

A.3.2 DNA Tracking Dye

Bromophenol blue (Saarchem)	62.5 mg
Sucrose (Saarchem)	10 g
EDTA (0.5 M, pH 8)	1 ml
dH_2O to	25 ml

Autoclave

A.3.3 MOPS buffer for RNA agarose-formaldehyde gels (10 X)

MOPS (Sigma)	20 g
Na Acetate (Saarchem)	1 g
EDTA (0.5 M, pH 8)	10 ml
DEPC- dH_2O	470 ml

Adjust pH to 7 with NaOH and filter sterilize through a 0.22 µm Millipore filter using a 60 cc syringe. A 1X solution of this was used as running buffer for RNA agarose gels. Store in the dark at 4 °C.

A.3.4 RNA sample buffer and gel tracking dye

MOPS (10 X) (pH 7)	300 ul
Formaldehyde (37 %) (Sarchem)	80 ul
Formamide (Saarchem)	900 ul
Ethidium Bromide (10 mg/ml) (Sigma)	2 ul
Dye	220 ul

The dye used was made up as follows:

Xylene cyanol (Saarchem)	50 mg
Bromophenol Blue (Saarchem)	50 mg
DEPC- dH_2O	1 ml

RNA Sample buffer was added at a ratio of 1:2 for RNA sample:sample buffer. The samples were then heated at 65 °C for 15 min, followed by snap cooling on ice before loading into gel wells.

A.4 Solutions for plasmid isolation

A.4.1 Antibiotics

Chloramphenicol (30 mg/ml)

Chloramphenicol (Roche)	30 mg
Ethanol	10 ml

Filter sterilize and store aliquots at 4 °C
Use 1 ml/L media

Ampicillin (100 mg/ml)

Ampicillin (Roche)	2 g
Water	20 ml

Filter sterilize and store aliquots at 4 °C.
Use 1 ml/L media

A.4.2 Solution 1 (10 X stock)

Tris-Cl (1 M, pH 8)	25 ml
Glucose (20 % w/v) (Saarchem)	45.5 ml
EDTA (0.5 M, pH 8)	20 ml
dH_2O	9.5 ml

A.4.3 Solution 2

NaOH (10 N) (Saarchem)	2 ml
SDS (25 %, w/v) (Saarchem)	4 ml
dH_2O	94 ml

This solution is made fresh weekly

A.4.4 Solution 3

K-acetate (Saarchem)	147 g
dH_2O to	250 ml

Adjust pH to 4.8 – 5.0 with Acetic acid. Make up to a final volume of 500 ml

A.5 Solutions for DNA isolation

A.5.1 Tris-EDTA (TE) buffer (pH 8) (1 M stock)

Tris-Cl (1 M, pH 8)	1 ml
EDTA (0.5 M, pH 8)	200 µl
dH_2O to	100 ml
Autoclave	

A.5.2 Sodium chloride (5M)

NaCl	29.22 g
dH_2O to	100 ml
Autoclave	

A.5.3 CTAB/NaCl

NaCl	4.1 g
CTAB	10 g
dH_2O to	100 ml

A.6 Solutions for RNA isolation

A.6.1 Diethylpyrocarbonate water (DEPC- dH_2O)

DEPC (Sigma)	1 ml
dH_2O	1 L

Shake solution vigorously until no DEPC droplets remain, and leave overnight in a fumehood
Autoclave

A.6.2 Anti-coagulation buffer (Gross *et al.*, 2001)

NaCl (0.45 M)	2.63 g
Glucose (0.1 M)	1.80 g
Sodium citrate (30 mM)	0.88 g
Citric acid (26 mM)	0.50 g
EDTA (10 mM)	0.30 g
DEPC-dH_2O to	100 ml

Adjust pH to 4.6 and autoclave

A.6.3 Lysis solution for RNA extraction (Chomczynski *et al.*, 1987)

Guanidium thiocyanate (4 M) (Sigma)	4.7 g
Sodium Citrate stock (1 M) (Saarchem)	0.25 ml
Sarkosyl stock (10 %, w/v) (Sigma)	0.5 ml
β-Mercaptoethanol (Merck)	70 ul
DEPC-dH_2O	9.18 ml

Filter sterilize before addition of β-Mercaptoethanol
Make up fresh before use

A.6.4 Sodium acetate (2M, pH 4)

Sodium acetate (trihydrate)	27.21 g
DEPC- dH_2O to	100 ml

Adjust to pH 4 with acetic acid
Autoclave

A.6.5 1.2% RNA Agarose Formaldehyde gel

Agarose	0.72 g
DEPC- dH_2O	43.92 ml

Let the solution cool to 60 °C, then add:

MOPS (10 X) (pH 7)	6 ml
Formaldehyde	10.08 ml

Pour gel and leave to set.

A.7 Solutions for MTT Assay

A.7.1 Acidic isopropanol

HCl (0.4 M)	2 ml
Isopropanol to	50 ml

A.8 Solutions for ATP Assay

A.8.1 Cell lysis buffer

Tris (20 mM)	0.05 g

NaCl (100 mM)	0.11 g
EDTA (1 mM)	0.075 g
Triton X-100 (0.5 %, Sigma)	1 ml
dH_2O to	20 ml
Autoclave before adding Triton-X-100	

A.8.2 10 mM EDTA

EDTA	0.93 g
PBS to	250 ml
Autoclave	

A.9 Solutions for NBT Assay

A.9.1 2 M KOH

KOH	2.24 g
dH_2O to	20 ml

A.10 Solutions for phagocytosis assay

A.10.1 0.1 M $NaHCO_3$ solution (pH 9.0)

$NaHCO_3$ (Saarchem)	0.84 g
dH_2O to	100 ml
Auitoclave	

A.10.2 EtBr 1mg/ml in PBS

EtBr (Sigma)	0.01 g
PBS	10 ml

APPENDIX B

CLONING VECTORS

CONTENTS

B.1 pDNR-LIB

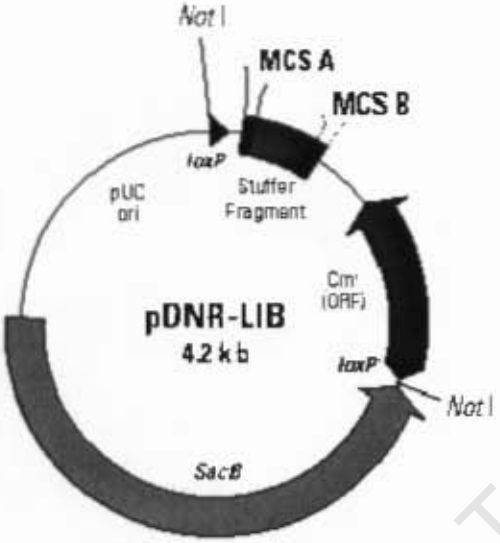

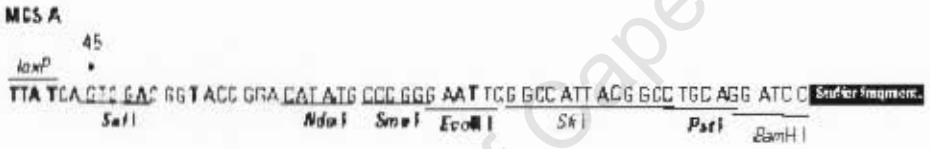

Diagram from Creator™ SMART™ cDNA Library Construction kit manual, (CLONTECH Laboratories, Inc.).

B.2 pGEM-T Easy Vector Cloning Vector

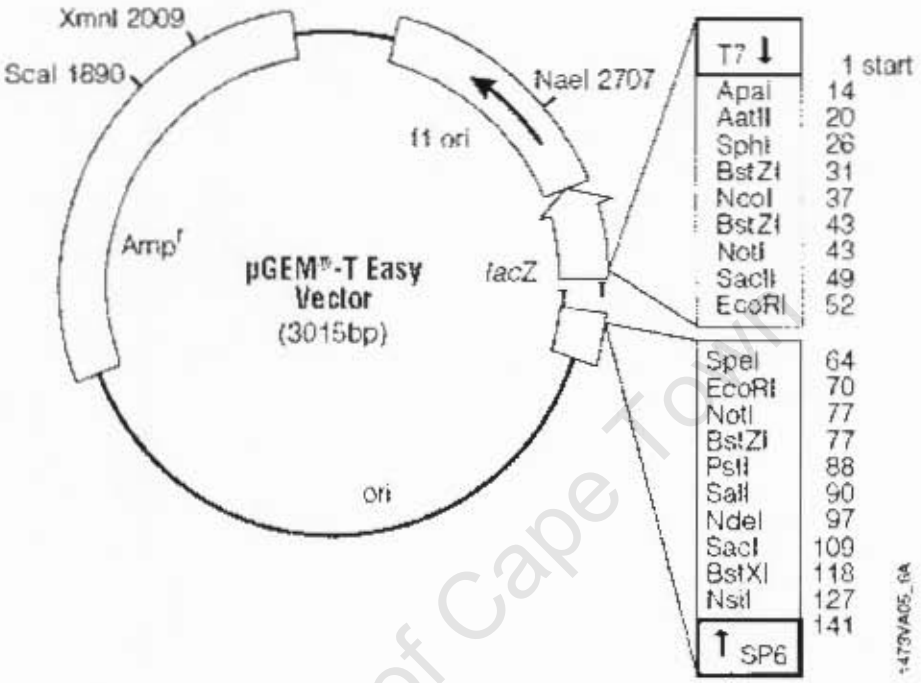

Diagram from pGEM®-T and pGEM®-T Easy Vector Systems Manual (Promega)

APPENDIX C

DNA PRIMER SEQUENCES, PCR CYCLE PROFILES AND cDNA CONVERSION CONDITIONS

CONTENTS

C.1 DNA PRIMER SEQUENCES

All synthetic oligonucleotide sequences were supplied by the Oligonucleotide synthesizing service of the Molecular and Cell Biology Department, University of Cape Town, Cape Town, South Africa.

C.1.1 Actin

ActF	5'	TGA CTA CCT CAT GAA GAT CC 3'
ActR	5'	CAT CTC CTG CTC AAA GTC G 3'

C.1.2 Cytochrome *b*

CytBF	5'	CGG ATT TGC GGT TGA TAA TGC 3'
CytBR	5'	CCA ATT CCT TCA TAC GCG GC 3'

C.1.3 Cytochrome *c* oxidase III (microarray clone)

CytCF	5'	TCT ACG TAG CCA CCG GAT TC 3'
CytCR	5'	TTG AGA GGT ACA GGA ATA GCC 3'

C.1.4 Cytochrome *c* oxidase III for 5' RACE

CoxC	5'	ACT ACG TGT AGG CCG TGG AAT CCG GTG GC 3'

C.1.5 M13 Universal (for sequencing)

M13F	5' CGC CAG GGT TTT CCC AGT CAC GAC 3'
M13R	5' GAG CGG ATA ACA ATT TCA CAC AGG 3'

C.2 PCR CYCLE PROFILES

C.2.1 Actin

1 cycle	denaturation	1 min	94 °C,
25 cycles	denaturation	30 s	94 °C
	annealing	30 s	60 °C
	elongation	1 min	72 °C
1 cycle	elongation	5 min	72 °C

C.2.2 Cytochrome *b*

1 cycle	denaturation	1 min	94 °C,
25 cycles	denaturation	30 s	94 °C
	annealing	30 s	60 °C
	elongation	1 min	72 °C
1 cycle	elongation	5 min	72 °C

C.2.3 Cytochrome *c* oxidase III

1 cycle	denaturation	1 min	94 °C,
22 cycles	denaturation	30 s	94 °C
	annealing	30 s	60 °C
	elongation	1 min	72 °C
1 cycle	elongation	5 min	72 °C

C.2.4 Cytochrome *c* oxidase III 5' RACE PCR

5 cycles	30 s	94 °C
	3 min	72 °C
5 cycles	30 s	94 °C
	30 s	70 °C
	3 min	72 °C
27 cycles	30 s	94 °C
	30 s	68 °C
	3 min	72 °C

C.3 CONDITIONS FOR cDNA CONVERSION

The conversion of RNA to cDNA was performed as instructed by the Impromp-II Reverse Transcriptase kit with some modifications. Briefly, $MgCl_2$, buffer, DNase and RNasin were added to 1 ug of template RNA as instructed by the kit and incubated for 90 min at 37 °C. After adding the stop buffer and OligodT, the samples were incubated for 5 min at 72 °C, 5 min at 4 °C and 5 minutes at room temperature. The dNTP and dH_2O was added and incubated for 5 minutes at 42 °C where after reverse transcriptase was added and incubated O/N at 42 °C. The RT was inactivated by incubating for 15 min at 70 °C. The cDNA was stored at -70 °C until used.

LITERATURE CITED

Abe K., Matzuki N. (2000) Measurement of cellular 3-(4,5-dimethylthiazol-2-yl)-2,5-diphenyltetrazolium bromide (MTT) reduction activity and lactate dehydrogenase release using MTT. *Neuroscience Research* **38**:325-329.

Allawi, H.T., Santa-Lucia, J. (1997) Thermodynamics and NMR of internal G-T mismatches in DNA. *Biochemistry*, **36**:10581-10594.

Bachère, E. (2003) Anti-infectious immune effectors in marine invertebrates: potential tools for disease control in marine larviculture. *Aquaculture* **227**:427-438.

Bachère, E., Mialhe, E., Noël, D., Boulo, V., Morvan, A., Rodrigues, J. (1995) Knowledge and research prospects in marine mollusc and crustacean immunology. *Aquaculture* **132**:17–32.

Balcazar J.L., de Blas I., Ruiz-Zarzuela I., Cunningham D., Vendrell D., Muzquiz J.L. (2006) The role of probiotics in aquaculture. *Veterinary Microbiology* **114**:173-186.

Barrientos A., Barros M.H., Valnot I., Rotig A., Rustin P., Tzagoloff A. (2002) Cytochrome oxidase in health and disease. *Gene* **286**:53-63.

Belyaeva E.A., Dymkowska D., Wieckowski M.R., Wojtczak L. (2006) Reactive oxygen species produced by the mitochondrial respiratory chain are involved in Cd^{2+} - induced injury of rat ascites hepatoma AS-30D cells. *Biochimica et Biophysica Acta* **1757**:1568-1574.

Bermudez R., Dagger F., D'Aquino A., Benaim G., Dawidowics K. (1997) Characterization of mitochondrial electron-transfer in *Leishmania mexicana. Molecular and Biochemical Parasitology* **90**:43-54.

Blecher M., Goldstein S. (1977) Hormone receptors: IV. On the nature of the binding of glucagon and insulin to human circulating mononuclear leukocytes. *Molecular and Cellular Endocrinology* **8(4)**:301-315.

Bouzidi M.F., Carrier H., Godinot C. (1996) Antimycin resistance and ubiquinol cytochrome *c* reductase instability associated with human cytochrome *b* mutation. *Biochimica et Biophysica Acta* **1317**:199-209.

Brousseau P., Pellerin J., Morin Y., Cyr D., Blakley B., Boermans H., Fournier M. (2000) Flow cytometry as a tool to monitor the disturbance of phagocytosis in the clam *Mya arenaria* hemocytes following in vitro exposure to heavy metals. *Toxicology* **142**:145-156.

Bugge D.M., Hegaret H., Wikfors G.H., Allam B. (2007) Oxidative burst in hard clam (*Mercenaria mercenaria*) haemocytes. *Fish & Shellfish Immunology* **23**:188-196.

Canesi L., Pruzzo C., Tarsi R., Gallo G. (2001) Surface interactions between *Escherichia coli* and hemocyte of the Mediterranean mussel *Mytilus galloprovincialis* Lam. leading to efficient bacterial clearance. *Applied and Environmental Microbiology* **67(1)**:464-468.

Canesi L., Scarpato A., Betti M., Ciacci C., Pruzzo C., Gallo G. (2002) Bacterial killing by *Mytilus* hemocyte monolayers as a model for investigating the signaling pathways involved in mussel immune defence. *Marine Environmental Research* **54**:547-551.

Cannino G., Di Liegro M., Di Liegro I., Rinaldi A.M. (2004) Analysis of cytochrome *c* oxidase subunits III and IV expression in developing rat brain. *Neuroscience* **128**:91-98.

Charlet M., Chernysh S., Philippe H., Hetru C., Hoffmann J.A., Bulet P. (1996) Isolation of several cysteine-rich antimicrobial peptides from the blood of a mollusk, *Mytilus edulis. J Biol Chem* **6:** 21808–21813.

Chena L., Segal D.M., Masha D.C. (2005) Semi-quantitative reverse-transcriptase polymerase chain reaction: an approach for the measurement of target gene expression in human brain. *Developmental Brain Research* **156(1)**:38-45.

Cheng H., Mai K., Zang W., Luifu Z., Xu W., Tan B. (2005) Effects of dietary pyridoxine on immune responses in abalone, *Haliotis discus discus. Fish and Shellfish Immunology* **19**:241-252.

Cheng T.C., Rodrick G.E., Foley D.A., Koehler S.A. (1975) Release of lysozyme from hemolymph of cells of *Mercenaria mercenaria* during phagocytosis. *Journal of Invertebrate Pathology* **25**:261-265.

Choi J.S., Kim J.W., Cha Y., Kim C. (2006) A quantitative nitroblue tetrazolium assay for determining intracellular superoxide anion production in phagocytic cells. *Journal of Immunoassays & Immunochemistry* **27**:31-44.

Chomczynski P., Sacchi N. (1987) Single-step method of RNA isolation by acid guanidium thiocyanate-phenol-chloroform extraction, *Analytical Biochemistry,* **162:**156-159

Chu F.E., Volety A.K., Hale R.C., Huang Y. (2002) Cellular responses and disease expression in oysters (*Crassostrea virginica)* exposed to suspended field – contaminated sediments. *Marine Environmental Research* **53**:17-53.

Cima F., Matozza V., Marin M.G., Ballarin L. (2000) Haemocytes of the clam *Tapes philippinarum* (Adams & Reeve, 1850): morphofunctional characterization. *Fish & Shellfish Immunology* **10**:677-693.

Cirelli C., Tononi G. (1998) Differences in gene expression between sleep and waking as revealed by mRNA differential display. *Molecular Brain Research* **56(1-2)**:293-305.

Dahlgren C., Karlsson A. (1999) Respiratory burst in human neutrophils. *Journal of Immunological Methods* **232**:3-14.

Fan W., Li C., Wang X., Gong N., Xie L., Zhang R. (2007) Cloning, characterization and expression analysis of calcium channel B subunit from Pearl Oyster (*Pinctada fucata*). *Journal of Bioscience and Bioengineering* **104(1)**: 47-54.

Felsenstein, J. (1985) Confidence limits on phylogenies: An approach using the bootstrap. *Evolution* **39**:783-791.

Fossati G., Moulding D.A., Spiller D.G., Moots R.J., White M.R.H., Edwards S.W. (2003) The mitochondrial network of human neutrophils: Role in chemotaxis, phagocytosis, respiratory burst activation and commitment to apoptosis. *The Journal of Immunology* **170**:1964-1972.

Fotakis G., Timbrell J.A (2006) In vitro cytotoxicity assays: Comparison of LDH, neutral red, MTT and protein assay in hepatoma cell lines following exposure to cadmium chloride. *Toxicology Letters* **160**:171-177.

Garnik E.Y., Tarasenko V.I., Kobsev V.F., Konstantinov Y.M. (2006) Differential expression of maize mitochondrial genes as dependent on mitochondria redox state. *Russian Journal of Plant Physiology* **53(4):**463-468.

Gesinki R.M. (1976) Effectiveness of antimycin A, oligomycin and sodium cyanide as inhibitors of rat bone marrow oxygen utilization. *Ohio Journal of Science* **76(3):**139-142.

Gomez-Gil, B., Roque, A., Turnbull, J. F. (2000) The use and selection of probiotic bacteria for use in the culture of larval aquatic organisms. *Aquaculture* **191**:259-270.

Gonzalez M., Romestand B., Fievet J., Huvet A., Lebart m., Gueguen Y., Bachere E. (2005) Evidence in oyster of a plasma extracellular superoxide dismutase which binds LPS. *Biochemical and Biophysical Research Communcations* **338**:1089-1097.

Gordon, H. R. and Cook, P. A. (2001) World abalone supply, markets and pricing: Historical, current and future. *Journal of Shellfish Research* **20(2)**:567-570.

Gram, L., Løvold, T., Nielsen, J., Melchiorsen, J., Spanggaard, B. (2001) In vitro antagonism of the probiotic *Pseudomonas fluorescens* strain AH2 against *Aeromonas salmonicida* does not confer protection of salmon against furunculosis. *Aquaculture* **199**:1–11.

Gross P., Bartlett T.C., Browdy C.L., Chapman R.W., Warr G.W. (2001) Immune gene discovery by expressed sequence tag analysis of haemocytes and hepatopancreas in the Pacific White Shrimp, *Litopenaeus vannamei,* and the Atlantic White Shrimp, *L. setferus, Developmental and Comparative Immunology,* **25:**565-577

Guo H., Wei J., Kuo P.C. (2001) Nitric oxide inhibits expression of cytochrome *b* in endotoxin-stimulated murine mactrophages. *Biochemical and Biophysical Research Communications* **289(5)**:993-997.

Hooper C., Day R., Slocombe R., Handlinger J., Benkendorff K. (2007) Stress and immune responses in abalone: Limitations in current knowledge and investigative methods based on other models. *Fish & Shellfish Immunology* **22**:363-379.

Hosler J.P. (2004) The influence of subunit III of cytochrome *c* oxidase on the D pathway, the proton exit pathway and mechanism-based inactivation in subunit I. *Biochimica et Biophysica Acta* **1655**:332-339.

Hong X., Xiang L., Shao J. (2006) Immunostimulating effect of bacterial genomic DNA on the innate responses of bivalve mussel *Hyriopsis cumingii.* Fish and Shellfish Immunology **21**(4): 357-364.

Hsieh M., Hsieh C., Lin L., Wu C., Huang G.S. (2003) Differential gene expression of scopolamine-treated rat hippocampus-application of cDNA microarray technology. *Life Sciences* **73**:1007-1016.

Jiravaichpaisal P., Puanglarp N., Petkon S., Donnuea S., Soderhall I., Soderhall K. (2007) Expression of immune-related genes in larval stages of the giant tiger shrimp, *Penaeus monodon. Fish & Shellfish Immunology* **23**:815-824.

Kaminska B., Kaczmarek L., Laroque S., Chaudhuri A (1997) Activity-dependent regulation of cytochrome *b* gene expression in monkey visual cortex. The Journal of Comparative *Neurology* **379**:279-282.

Khalimonchuk O., Rodel G. (2005) Biogenesis of cytochrome *c* oxidase. *Mitochondrion* **5**:363-388.

Knauer, J., Britz, P. J., Hecht, T. (1996) Comparative growth performance and digestive activity of juvenile South African abalone, *Haliotis midae*, fed diatoms and a practical diet. *Aquaculture* **140**:75–85.

Kobzik L., Godleski J.J., Brain J.D. (1990) Selective down-regulation of alveolar macrophage oxidative response to opsonin-independent phagocytosis. *Journal of Immunology* **144(11)**:4312-4319.

Ksenzenko M., Konstantitov A.A., Khomutov G.B., Tikhonov A.N., Ruuge E.K. (1983) Effect of electron transfer inhibitors on superoxide generation in the cytochrome *bc*1 site of the mitochondrial respiratory chain. *FEBS Letters* **155(1)**:19-24.

Kumar K.T., Nei M. (2004) MEGA3: Integrated software for Molecular Evolutionary Genetics Analysis and sequence alignment. *Briefings in Bioinformatics* **5**:150-163.

Labreuch Y., Lambert C., Soudant P., Boulo V., Huvet A., Nicolas J. (2006) Cellular and molecular haemocyte responses of the Pacific oyster, *Crassostrea gigas*, following bacterial infection with *Vibrio aestuarianus* strain 01/32. *Microbes and Infection* **9**:2715-2724.

Lacoste, A., Malham, S. K., Gélébart, F., Cueff, A., Poulet, S. A. (2002) Stress-induced immune changes in the oyster *Crassostrea gigas. Developmental and Comparative Immunology* **26**:1–9

Li H., Haberzettl P., Albrecht C., Hohr D., Knaapen A.M., Borm P.J.A., Schins R.P.F. (2007) Inhibition of the mitochondrial respiratory chain function abrogates quartz induced DNA damage in lung epithelial cells. *Mutation Research* **617**:46-57.

Li H.Y., Dai L.J., Quamme G.A (1993) Effect of chemical hypoxia on intracellular ATP and cytosolic Mg^{2+} levels. *Journal of Laboratory Clinical Medicine* **122(3):**260-272.

Lienard M.A., Lassance J.X.S., Paulmier I., Picimbon J., Lofstedt C. (2006) Differential expression of cytochrome *c* oxidase subunit III gene in castes of the termite *Reticulitermes santonensis*. Journal of Insect Physiology 52:551-557.

Ling E., Yu X. (2006) Hemocytes from the tobacco hornworm *Manduca sexta* have distinct functions in phagocytosis of foreign particles and self dead cells. *Developmental and Comparative Immunology* **30**:301-309.

Lobner D. (2000) Comparison of the LDH and MTT assays for quantifying cell death: validity for neural apoptosis? *Journal of Neuroscience Methods* **96**:147-152.

Macey B.M (2005) Probiotic effect of *Vibrio midae* SY9, *Cryptococcus* sp. SS1 and *Debaryomyces hansenii* AY1 on the growth and disease resistance of farmed *Haliotis midae.* University of Cape Town, Cape Town.

Macey, B. M., Coyne, V. E. (2005) Improved growth rate and disease resistance in farmed *Haliotis midae* through probiotic treatment. *Aquaculture* **242**:249-261.

Malham, S. K., Lactose, A., Gélébart, F., Cueff, A., Poulet, S. A. (2003) Evidence for a direct link between stress and immunity in the mollusk *Haliotis tuberculata. J. Exp. Zoo.* **295A**:136–144

Marquis R.E. (1965) Nature of the bactericidal action of antimycin A for *Bacillus megaterium. Journal of Bacteriology* **89(6):**1453-1459.

Matsuno-Yagi A., Hatefi Y. (1999) Ubiquinol:Cytochrome *c* oxidoreductase: Effects of inhibitors on reverse electron transfer from the iron-sulfur protein to cytochrome *b*. *The Journal of Biological Chemistry* **274(14):**9263-9288.

Matricon M., Letocart M. (1999) Internal defense of the snail *Biomphalaria glabrata* I: Characterisation of haemocytes and fixed phagocytes. *Journal of Invertebrate Pathology* **74**:224

Meany D.L, Poe B.G., Navratil M., Moraes C.T., Arriaga E.A. (2006) Superoxide released into the mitochondrial matrix. *Free Radical Biology & Medicine* **41**:950-959.

Mialhe, E., Bachére, E., Boulo, V., Cadoret, J. P. (1995) Strategy for research and international cooperation in marine invertebrate pathology, immunology and genetics. *Aquaculture* **132**:33–41.

Miller T.E. (1971) Metabolic event involved in the bactericidal activity of normal mouse macrophages. *Infection and Immunity* **3(3)**:390-397.

Miyazaki T., Neff L., Tanaka S., Horne W.C., Baron R. (2003) Regulation of cytochrome *c* oxidase activity by c-Src in osteoclasts. *The Journal of Cell Biology* **160(5)**:709-718.

Molinari BL., Tasat D.R., Palmieri M.A., Cabrini R.L. (2005) Kinetics of MTT-formazan exocytosis in phagocytic and non-phagocytic cells. *Micron* **36**:177-183.

Mukhopadhyay P., Rajesh M., Yoshihiro K., Hasko G., Pacher P. (2007) Simple quantitative detection of mitochondrial superoxide production in live cells. *Biochemical and Biophysical Research Communication* **358**:203-208.

Munoz M., Cedeno R., Rodriquez J., van der Knaap W.P.W., Mialhe E., Bachere E. (2000) Measurement of reactive oxygen intermediate production in haemocytes of the penaeid shrimp, *Penaeus vannamei. Aquaculture* **191**:89-107.

Murray A.G., Peeler E.J. (2005) A framework for understanding emerging diseases in aquaculture. *Preventative Veterinary Medicine* **67**:223-235.

Niknahad H., Khan S., O'Brien P.J. (1995) Hepatocyte injury resulting from the inhibition of mitochondrial respiration at low oxygen concentrations involves reductive stress and oxygen activation. *Chemico-Biological Interactions* **98**:27-44.

Niknahad H., Khan S., O'Brien P.J. (1995b) Oxygen dependence of hepatocyte susceptibility to mitochondrial respiratory inhibitors. *Biochemical Pharmacology* **39(11)**:1859-1965.

Oh J., Jeon Y., Jeong S., Hong S. M., Lee J.S., Nho S.K., Kang S.W., Kim N. (2006) Gene expression profiling between embryonic and larval stages of the silkworm, *Bombyx mori. Biochemical and Biophysical Research Communication* **343**:864-872.

Ohta M., Watanabe A., Mikami T., Nakajima Y., Kitami M., Tabunoki H., Ueda K., Sato R. (2006) Mechanism by which *Bombyx mori* hemocytes recognize microorganisms: direct and indirect recognition systems for PAMPs. *Developmental and Comparative Immunology* **30**:867-877.

Paraonu L.E., Wei B., Robitzki A.A., Layer P.G. (2005) Cytochrome *c* oxidase is one of several genes elevated in marginal retina of the chick embryo. *Neuroscience* **132(3):**665-672.

Park W., Han Y., Kim S.W, Kim S.H, Cho K., Kim S.Z. (2007) Antimycin A induces apoptosis in As4.1 juxtaglomerular cells. *Cancer Letters* **251**:68-77.

Petrosillo G., Ruggiero F.M., Venosa N.D., Paradies G. (2003) Decreased complex III activity in mitochondria isolated from rat heart subjected to ischemia and reperfusion: role of reactive oxygen species and cardiolipin. *The FASEB Journal* **17**:714-716.

Read P., Fernandez T. (2003) Management of environmental impacts of marine aquaculture in Europe. *Aquaculture* **226**:139-163.

Reddy-Lopata K., Auerswald L., Cook P. (2006) Ammonia toxicity and its effects on the growth of the South African abalone *Haliotis midae* Linnaeus. *Aquaculture* **261**:678-687.

Reiss M., Roos D. (1987) Differences in oxygen metabolism of phagocytosing monocytes and neutrophils. *The Journal of Clinical Investigation* **61**:480-488.

Richter O.M., Ludwig B. (2003) Cytochrome *c* oxidase – structure, function and physiology of a redox-driven machine. *Review of Physiological and Biochemical Pharmacology* **147**:47-74.

Rieske J.S., Lipton S.H., Baum H., Silman H.I. (1967) Factors affecting the binding of antimycin A to complex III of the mitochondrial respiratory chain. *The Journal of Biological Chemistry* **242(21)**:4888-4896.

Robalino J., Bartlett T.C., Chapman R.W., Gross P.S., Browdy C.L., Warr G.W. (2007) Double-stranded RNA and antiviral immunity in marine shrimp: Inducible host mechanisms and evidence for the evolution of viral counter-responses. *Developmental and Comparative* Immunology **31**:539-547.

Roch, P. (1999) Defence mechanisms and disease prevention in farmed marine invertebrates. *Aquaculture* **172**:125–145.

Rychlik, W., Spencer W.J., Rhoads R.E. (1990) Optimization of the annealing temperature for DNA amplification in vitro. *Nucleic Acids Research* **18**:6409-6412.

Saitou, N., Nei, M. (1987) The neighbour-joining method: A new method for reconstructing phylogenetic trees. *Molecular Biology and Evolution* **4**:406-425.

Sambrook, J., Fritsch, E. F. and Maniatis, T. 1989. *Molecular cloning.* A laboratory manual, (2nd edition), Cold Spring Harbor Laboratory Press, Cold Spring Harbor, New York.

Sandeep R., McEachern G.E., Myint A.T., Robinson B.H. (2000) Superoxides from mitochondrial complex III: The role of manganese superoxide dismutase. *Free Radical Biology & Medicine* **29(2)**:170-180.

Sas K., Robotka H., Toldi J., Vecsei L. (2007) Mitochondria, metabolic disturbances, oxidative stress and the kynurenine system, with focus on neurodegenerative disorders. *Journal of Neurological Sciences* **257**:221-239.

Sbarra A.J., Karnovsky M.L. (1959) The biochemical basis of phagocytosis. *The Journal of Biological Chemistry* **234**(6):1355-1362.

Schultz B.E., Chan S.I. (2001) Structures and proton-pumping strategies of mitochondrial respiratory enzymes. Annual *Review of Biophysics and Biomolecular Structure* **20**:23-65.

Sierra C., Lascurain R., Pereyra A., Guevara J., Martinez G., Agundis C., Zenteno E., Vazquez L. (2005) Participation of serum and membrane lectins on the oxidative burst regulation in *Macrobrachium rosenbergii* hemocytes. *Developmental and Comparative Immunology* **29**:113-121.

Siraki A.G., Pourahmad J., Chan T.S., Khan S., O'Brien P.J. (2002) Endogenous and endobiotic induced reactive oxygen species formation by isolated hepatocytes. *Free Radical Biology & Medicine* **32(1)**:2-10.

Song L., Zou H., Chang Y., Xu W., Longtao W. (2006) The cDNA cloning and mRNA expression of a potential selenium-binding protein gene in the scallop *Chlamys farreri*. *Developmental and Comparative Immunology* **30**:265-273.

Soria F., Sierra C., Bouquelet S., Brassart C., Agundis C., Zenteno E., Vazquez L. (2006) The effect of sugars and free amino acids from the freshwater prawn *Macrobrachium rosenbergii* hemolymph on lectin activity and on oxidative burst. *Comparative Biochemistry and Physiology, Part C* **142**:212-219.

Stevens M.M (2003) Cultured abalone (*Haliotis* spp.). Monterey Bay Aquarium Seafood Watch ® Seafood Report. Retrieved on 22 April 2007 from www.seafoodwatch.org

Tanaka R., Ootsubo M., Sawabe T., Ezura Y., Tajima K. (2004) Biodiversity and in situ abundance of gut microflora of abalone (*Haliotis discus hannai*) determined by culture-independent techniques. *Aquaculture* **241**:453-463.

Tanguy A., Guo Z., Ford S.E. (2004) Discovery of genes expressed in response to *Perkinsus marinus* challenge in Eastern (*Crassostrea virginica*) and Pacific (*C. gigas*) oysters. *Gene* **338**:121-131.

Tazawa E., Fujiwara A., Ishida O., Yasumasu I. (1996) Photoactivation of NADH cytochrome *c* reductase in mitochondria isolated from sperm, eggs and viscera of sea urchin, oyster, abalone and echiuroid. *Comparative Biochemistry and Physiology Part B: Biochemistry and Moleculary Biology* **114** (3):245-250.

Terenius O., Bettencourt R., Lee S.Y., Li W., Soderhall K., Faye I. (2007) RNA interference

of *Hemolin* causes depletion of phenoloxidase activity in *Hyalophora cecropia*. *Developmental and Comparative Immunology* **31**:571-575.

Thompson, J.D., Gibson, T.J., Plewniak, F., Jeanmougin, F., Higgins, D.G. (1997) The ClustalX windows interface: flexible strategies for multiple sequence alignment aided by quality analysis tools. *Nucleic Acids Research*, **25**:4876-4882.

Tian H., Vinson S.B., Coates C.J. (2004) Differential gene expression between alate and dealate queens in the red imported fire ant, *Solenopsis invicta* Buren (Hymenoptera: Formicidae). *Insect Biochemistry and Molecular Biology* **34**:937-949.

Tjensvoll K., Hodneland K., Nilsen F., Nylund A. (2005) Genetic characterization of the mitochondrial DNa from *Lepeophtheirus salmonis* (Crustacea; Copepoda). A new gene organization revealed. *Gene* **353**:218-230.

Troell M., Robertson-Andersson D., Anderson R.J., Bolton J.J., Maneveldt G., Halling C., Probyn T. (2006) Abalone farmng in South Africa: An overview with perspectives on kelp resources, abalone feed, potential for on-farm seaweed production and socio-economic importance. *Aquaculture* **257**:266-281.

Volety, A. K., Oliver, L. M., Genthner, F. J., Fisher, W. S. (1999) A rapid tetrazolium dye reduction assay to assess the bactericidal activity of oyster (*Crassostrea virginica*) haemocytes against *Vibrio parahaemolyticus*. *Aquaculture* **172**:205-222.

Vrbacky M., Drahota Z., Mracek T., Vojitiska A., Jesina P., Stopka P., Houstek J. (2007) Respiratory chain components involved in the glycerophosphate dehydrogenase-dependent ROS production by brown adipose tissue mitochondria. *Biochimica et Biophysica* **1767**:989-997.

Watabe M., Nakaki T. (2007) ATP depletion does not account for apoptosis induced by inhibition of mitochondrial electron transport chain in human dopaminergic cells. *Neuropharmacology* **52**:546-541.

Wolvetang E.J., Johnson K.L., Krauer K., Ralph S.J., Linnane A.W. (1994) Mitochondrial respiratory chain inhibitors induce apoptosis. *FEBS Letters* **339**: 40-44.

Wongprasert K., Sangsuriya P., Phongdara A., Senapin S. (2007) Cloning and characterization of a caspase gene from black tiger shrimp (*Penaeus monodon*)-infected with white spot syndrome virus (WSSV). *Journal of Biotechnology* **131**:9-19.

Wootton E.C., Dyrynda E.A., Pipe R.K., Ratcliffe N.A. (2003) Comparisons of PAH-induced immunomodulation in three bivalve molluscs. *Aquatic Toxicology* **65**:13-25.

Wootton E.C., Pipe R.K. (2003) Structural and functional characterization of the blood cells of the bivalve mollusk, *Scrobicularia plana*. *Fish & Shellfish Immunology* **15**:249-262.

Yin S., He J.Y., Gong Z., Lam T.J., Sin Y.M (1999) Identification of differentially expressed genes in Con A-activated Carp (*Cyprinus carpio* L.) leucocytes. *Comparative Biochemistry and Physiology Part B: Biochemistry and Molecular Biology* **124**:31-50.

Young F.M., Phungtamdet W., Sanderson B.J.S. (2005) Modification of MTT assay conditions to examine the cytotoxic effects of amitraz on the human lymphoblastoid cell line, WIL2NS. *Toxicology in Vitro* **19**:1051-1059.

Zelck U.E., Janje B., Scheider O. (2005) Superoxide dismutase expression and H_2O_2 production by hemocytes of the trematodie intermediate host *Lymnaea stagnalis* (Gastropoda). *Developmental and Comparative Immunology* **29**:305-314.

Zhang J., Tirmenstein M.A., Nicholls-Grzemski F.A., Fariss M.W. (2001) Mitochondrial electron transport inhibitors cause lipid peroxidation-dependent and –independent cell death: protective role of antioxidants. *Archives of Biochemistry and Biophysics* **393** (1):87-96.